DESIGN AND SYNTHESIS OF A FLUORESCENT CHEMODOSIMETER FOR THE ANALYSIS OF THE GOLD IONS

A Thesis Submitted to
the Graduate School of Engineering and Sciences of
İzmir Institute of Technology
in Partial Fulfillment of the Requirements for the Degree of

MASTER OF SCIENCE

in Chemistry

by
Merve ÇEVİK EREN

December 2018
İZMİR

We approve the thesis of **Merve ÇEVİK EREN**

Examining Committee Members:

Assoc. Prof. Dr Mustafa EMRULLAHOĞLU
Department of Chemistry, İzmir Institute of Technology

Assoc. Prof. Dr YAŞAR AKDOĞAN
Department of Materials Science and Engineering, İzmir Institute of Technology

Asst. Prof. Dr Nesrin HORZUM POLAT
Department of Engineering Science, İzmir Katip Çelebi University

27 December 2018

Assoc. Prof. Dr Mustafa EMRULLAHOĞLU
Supervisor, Department of Chemistry
İzmir Institute of Technology

Prof. Dr Ahmet Emin EROĞLU
Head of Department of Chemistry

Prof. Dr Aysun SOFUOĞLU
Dean of the Graduate School of
Engineering and Sciences

ACKNOWLEDGMENTS

First of all, there are many people to thank. I am heartily thankful to my supervisor Assoc. Prof. Dr Mustafa EMRULLAHOĞLU for his patient guidance, encouragement and excellent advice not only throughout this study but also in my life. This thesis could not have been written without his astute guidance.

It was an honor to study with him. During this work, I have worked together with my colleagues Erman Karakuş, Canan Üçüncü, Melike Sayar, Suay Dartar. I would like to thank all those who have helped me with my work in the laboratory.

Special thanks to Assoc. Prof. Dr Yaşar AKDOĞAN and Asst. Prof. Dr Nesrin HORZUM POLAT participating as a committee member and for reviewing my work.

I am deeply and forever indebted to my parents for their love, support and encouragement throughout my entire life especially Ahmet EREN.

ABSTRACT

DESIGN AND SYNTHESIS OF A FLUORESCENT CHEMODOSIMETER FOR THE ANALYSIS OF THE GOLD IONS

The gold element has been used in many different areas throughout history. This includes the treatment of various diseases with drugs containing gold. In contrast to gold metal, gold ions are known to be extremely harmful to the human body. Therefore, the determination of the gold ions in the human body is very important.

Gold ion determination can be made by using expensive spectroscopic methods. In contrast to highly expensive spectroscopic methods, chemosensors with high sensitivity and selectivity are a good option to make the gold determination. The bodipy fluorophore is a good example for the metal ion chemosensor. In this study, a bodipy-based fluorescence sensor derived from a unique motif that has a triple bond was designed and synthesized. By activating the triple bond of the gold ions, it becomes selective to the gold ions as a result of ırreversible intramolecular cycling.

ÖZET

ALTIN İYONLARININ ANALİZİ İÇİN BİR FLORESAN KEMODOSİMETRENİN TASARIM VE SENTEZİ

Altın elementi tarihte birçok farklı alanda kullanılmıştır. Altın elementi yapısında altın içeren birtakım ilaçlarla çeşitli hastalıkların tedavisinde de kullanılır. Altın metalinin aksine altın iyonlarının insan vücuduna son derece zararlı olduğu bilinmektedir. Bu nedenle insan vücudunda altın iyonlarının tayini oldukça önemlidir.

Pahalı spektroskopik yöntemler kullanılarak altın iyonu tayini yapılabilmektedir. Oldukça pahalı spektroskopik yöntemlerin aksine duyarlılığı ve seçiciliği yüksek olan kemosensörler altın tayini yapmak için iyi bir seçenektir. Bu nedenle, bodipy floroforu metal iyon kemosensörü için oldukça iyi bir örnektir. Bu çalışmada, yapısında üçlü bağ barındıran özgün bir motif ile türevlenmiş bodipy bazlı floresan algılayıcı tasarlanmış ve sentezlenmiştir. Altın iyonlarının üçlü bağı aktive ederek geri dönüşümü olmayan molekül içi halkalaşması sonucu altın iyonlarına seçici hale gelmiştir.

TABLE OF CONTENTS

LIST OF FIGURES

ABBREVIATIONS

BODIPY	3,5-Diaryl-4,4-difluoro-4-bora-3a,4a-diaza-s-indacene
DCM	Dichloromethane
DDQ	2,3-Dichloro-5,6-dicyano-1,4-benzoquinone
DIPEA	Diisopropylethylamine
EtOH	Ethanol
g	Grams
h	Hour
M	Molar
MeCN	Acetonitrile
MeOH	Methanol
mg	Miligrams
min.	Minute
mL	Mililiter
mmol	Milimoles
NEt_3	Triethylamine
NIS	N-Iodosuccinimide
nm	Nanometer
NMR	Nuclear Magnetic Resonance
ON	Overnight
PBS	Phosphate buffered saline
RT	Room temperature
THF	Tetrahydrofuran
TMS	Trimethylsilylacetylene
TMSCl	Trimethylsilyl chloride
TLC	Thin Layer Chromatography

CHAPTER 1

INTRODUCTION

1.1. History and usage of gold

Natural gold was found in Spanish caves in 4000 BC. Gold has attracted people's attention during every period of history because of its softness, making it easy to take shape without any difficult operation, and the fact that it almost never loses its bright yellow colour. For this reason, gold is used in many places today like in the fields or dentistry and medicine, and as a conductor. It is also used in biological activities.

Gold was used in dentistry for nearly 3000 years. Dentists filled cavities and rotten teeth with gold leaf. It was used in medical fields such as treating furuncles, skinning ulcers and removing mercury from the skin. Gold is a very efficient electrical conductor and is used in most electronic devices especially in mobile phones.

Metallic gold is non-toxic and stable. Ionic gold, however, is toxic, air-sensitive, and water soluble. An atom of ionic gold is essentially an atom of gold missing three electrons. It is the outermost layer of an atom, the one containing its electrons,that determines its physical properties. For this reason, the ionic form of gold reacts with other elements and is unstable. On the other hand, metallic gold does not react with other elements and stable.

Gold toxicity is the term that denotes gold’s effect on the human body. Gold is sometimes prescribed for rheumatoid arthritis (RA), juvenile rheumatoid arthritis (JRA), or psoriatic arthritis. When applied to the skin near a joint, gold can reduce pain and swelling. Gold treatment helps to reduce joint deformity and discomfort. However, the long-term effects of gold toxicity include liver inflammation, a blue-grey colour of the skin, and mouth ulcers.

Small gold levels are common in the environment. However, large amounts of gold can cause acute or chronic toxicity. Therefore, being able to determine the number of gold ions in the human body is very important. Trace amounts of gold can be found using spectroscopic methods such as atomic absorption and atomic emission

spectroscopy. However, these spectroscopic methods are expensive and time-consuming. In contrast to these methods, identifying trace amounts of gold by fluorogenic and chromogenic methods with high sensitivity and selectivity has been a good alternative. In these methods, the samples are more easily prepared and simpler devices are used (Das et. al, 2011).

1.2. Bodipy as fluorophore and its properties

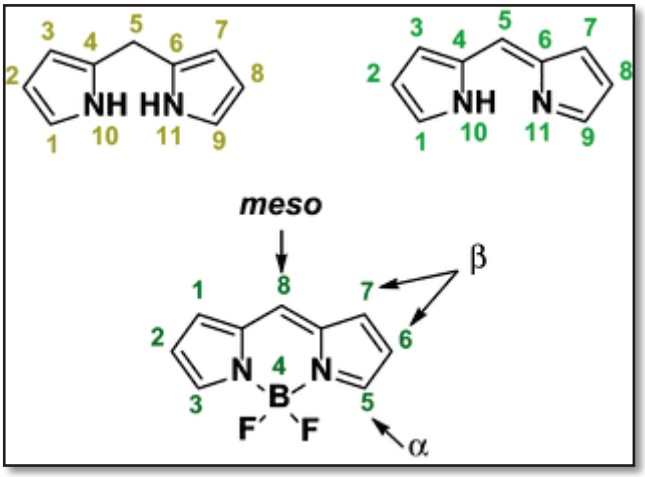

Figure 1.1. Structure of bodipy

Bodipy dyes have been used more and more often among fluorescent organic compounds in the last 20 years, and they are still being studied. Since the first Bodipy paint was reported by Treibs and Kreuzer (Treibs and Kreuzer 1968), many different Bodipy dyes have been synthesized and used in various applications. These dyes are insoluble or only slightly soluble in water. Their solubility in organic solvents is due to their fortuitous molecular structures. 8-Phenyl Bodipy is the most studied structure among them. As long as the conjugated groups are not attached to the chromophore group, most forms of Bodipy have a maximum absorption of 500-515 nm and a maximum emission within the range of 515-535 nm. .(Loudet et. al, 2007).

The various synthesized Bodipy derivatives have shown strong fluorescence, sharp absorption, and emission peaks similar to each other. Absorption and emission peaks shift to a red wavelength with increasing substituents in structure. The substituents

at position 8 do not change much in their fluorescence properties. When bulky groups were attached to the 1.7 or 3.5 positions in the pyro-pyric unit, there was a decrease in the intensity of the fluorescence

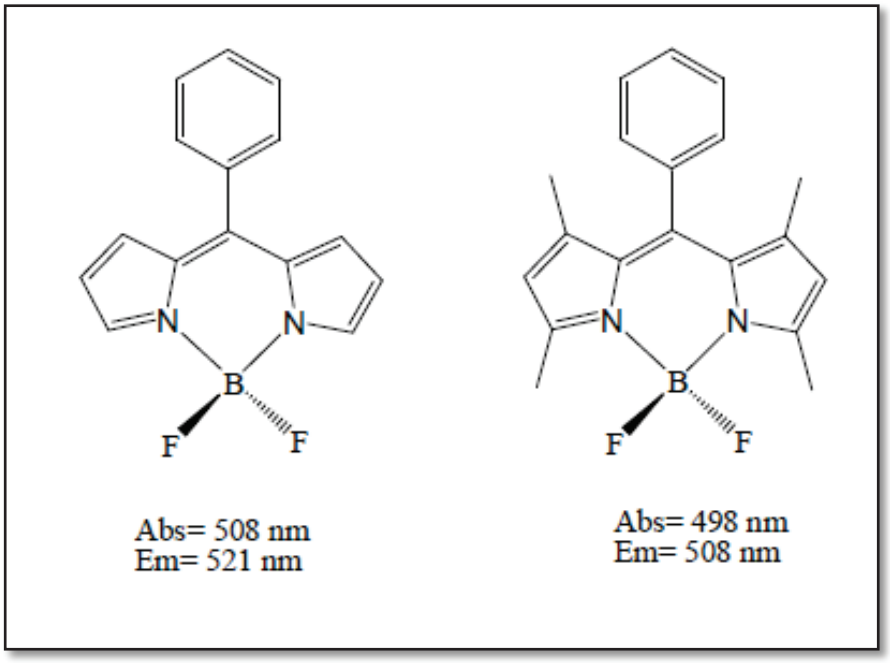

Figure 1.2. The effect of bulky alkyl substituents on Aril Bodipy at positions 1.7.

Recently, various studies have been carried out on the applications, reactions, and synthesis of the Bodipy molecule in fluorescent chemosensors. Bodipy can be used to detect changes in metal cations, anions, reactive oxygen species, and even viscosity by changes in fluorescence intensity and wavelength. These changes are usually controlled by an ON / OFF switch, starting and stopping the photo-induced electron transfer between Bodipy and the 8-phenyl substituent. Recently, the singlet oxygen producing groups of Bodipy derivatives were used as a photodynamic therapy agent.

They are also commonly combined with porphyrins and phthalocyanines. (Ozlem and Akkaya et al., 2009). Recently, interest in photonic organic based materials has increased. Bodipy develops as an extremely important unit of this class of compounds that demonstrate energy transfer through the new laser behaviour and highly effective bond and through space.

As a result, the application areas can be listed as follows; photodynamic therapy agents, energy transfer cassettes, colour-sensitive solar cells, chemosensor for metal cations, polymers, active fluorophor in the chemosensor field and laser dyes.

CHAPTER 2

LITERATURE WORKS

2.1. Ratiometric probe for gold ion

In 2010, Peng published a highly selective ratiometric fluorescent probe for Hg^{2+} or Au^{3+} in aqueous media, depending on reaction conditions. Using pH adjustment in different aqueous solutions, a nonsulfide probe based on a 1,8-naphthalimide and alkyne conjugate was developed for ratiometric fluorescence detection for Hg^{2+} and Au^{3+}. In this study, unlike in others, the probe worked at ph 9. The probe showed the dual character in different pH in aqueous media. This study also provides a novel sulfonide approach for selective recognition of these two ions. (Figure 2.1.)

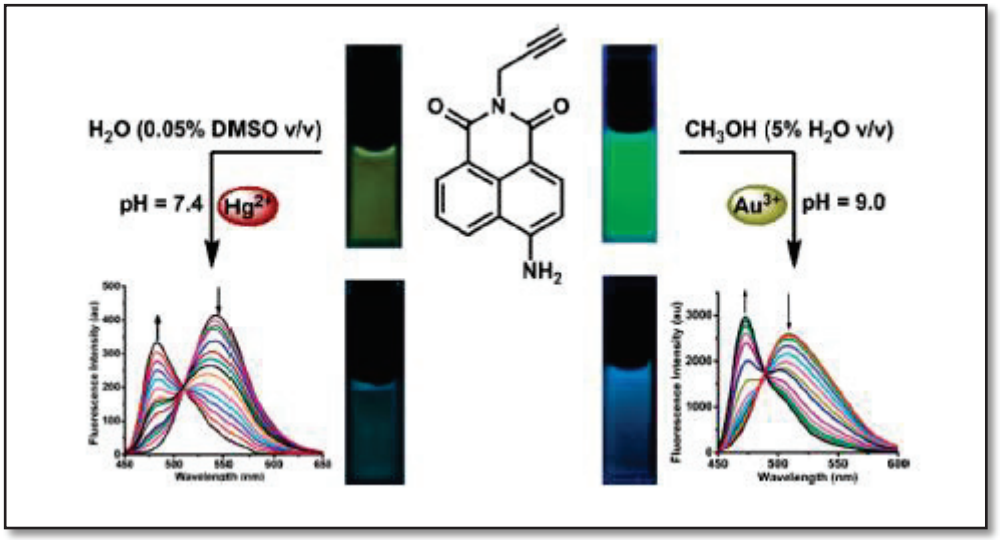

Figure 2.1. Highly Selective Ratiometric Fluorescent Sensing for Hg^{2+} and Au^{3+}, in Aqueous Media (Source: Peng et al., 2010).

In 2011, Cao reported the first FRET-based ratiometric fluorescent gold probe capable of quantitative determination of gold ions and nanoparticles. In this research, BODIPY dye was combined with rhodamine dye. The choice of BODIPY dye is based

on the idea that the emission of the BODIPY fluorophores coincides perfectly with the absorption of the rhodamine dye release form. Thus, the combination of BODIPY dye and rhodamine fluorophore is a suitable FRET dyad. For the very first time in the literature and, specifically, the quantitative detection of gold nanoparticles, (Figure 2.2).(Cao et.al.,2011)

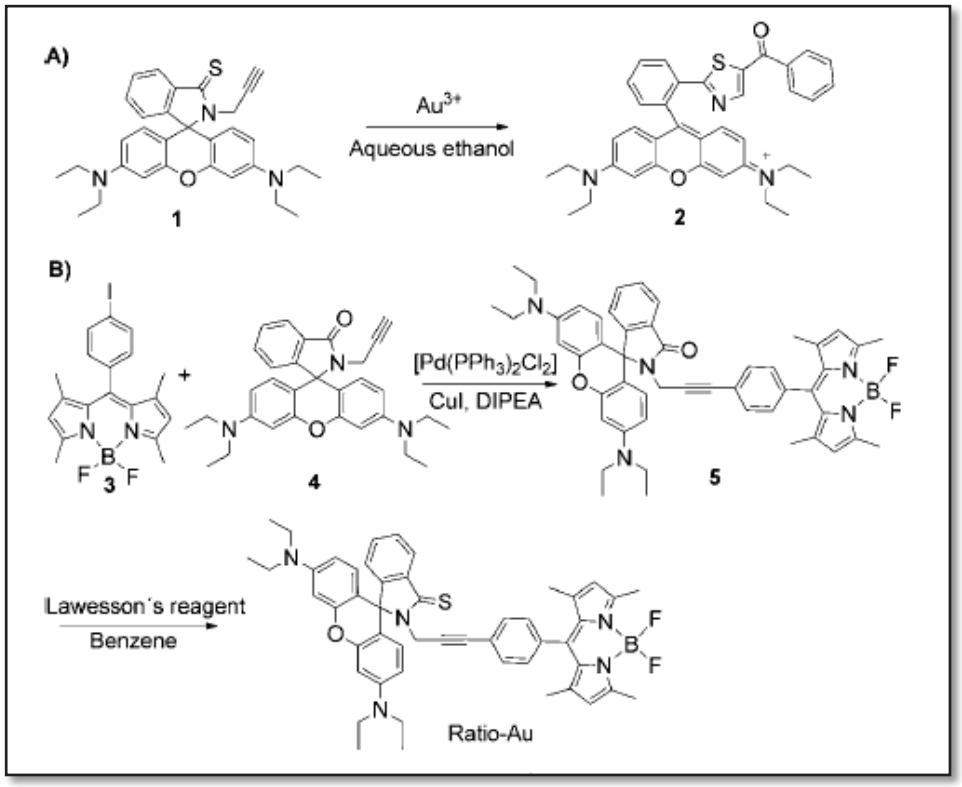

Figure 2.2. Ratio-Au: A FRET-based Fluorescent Probe for Ratiometric Determination of Gold Ions and Nanoparticles(Source: Cao et al., 2011).

The probe showed high sensitivity and selectivity to Au^{3+}. The 4-propargylamino-1,8-naphthalimide-based fluorescent probe for selective detection of gold ions was designed by Choi et al. (2013). Generally, 4-amino-1,8-naphthalimides having typical ıntramolecular charge transfer (ICT) electronic properties are commonly used as multidirectional platforms for fluorescent probes. The most important feature of these probes is that the substances that promote the strengthening or attenuation of the "push-pull"electronic nature of the 4-amino-naphthalimide group can be used to detect substances that cause a blue or red shift in their emissions.

In the presence of a gold ion, the probe colour shifts from yellow to light pink. Results of studies investigating the application of Au^{3+} in the bioimaging of living cells show that the probe has the ability to detect Au^{3+} in lipid droplets in cells. (Figure 2.3).(Choi et.al.,2013)

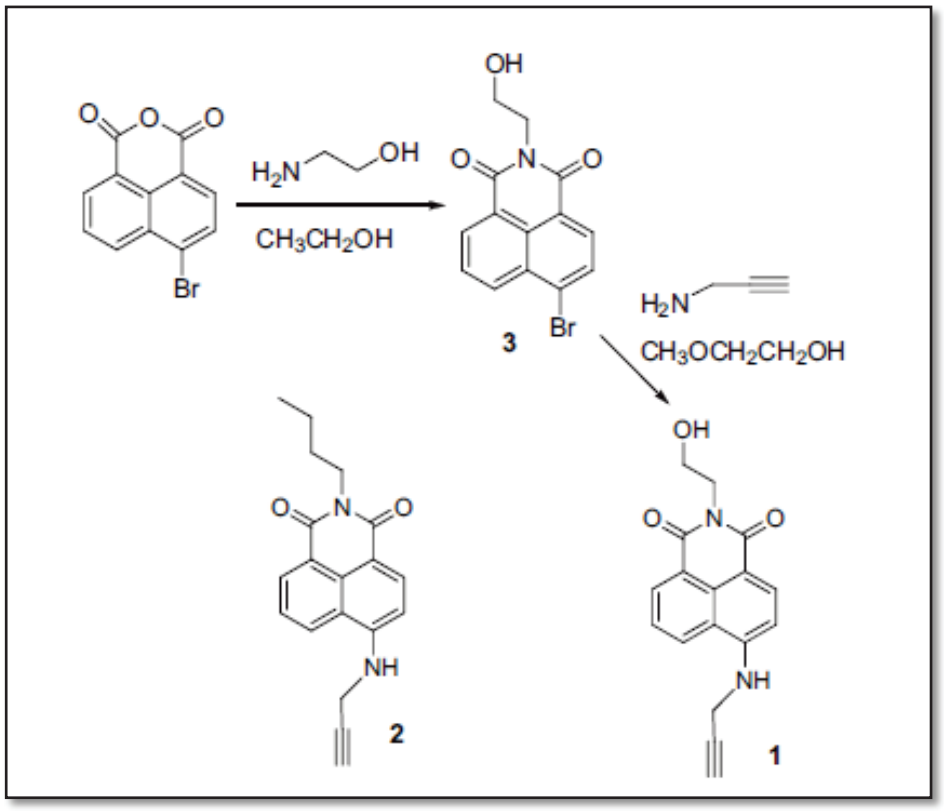

Figure 2.3. Highly selective ratiometric fluorescent probe for Au3+and its application to bioimaging.).(Source: Choi et.al.,2013)

In 2015, Wang and colleagues designed and synthesized a mono-Schiff-base fluorescent probe based on a boron-dipyrromethene (BODIPY) dye. They described two types of fluorescent probes. The BODIPY fluorophore was derivatized with 2-hydrazino pyrazine and 2-acetyl pyrazine groups as the metal ion recognition motif. This probe generally includes non-common C=N bonds that are nonfluorescent. In the presence of a gold ion, the irreversible hydrolysis reaction of C=N bond occurs. Comparing the two probes, probe 1 has pH and temperature stability, a low detection limit, and rapid response. It was also successfully applied to zebrafish imaging with excellent cell-membrane permeability and organism permeability. (Figure 2.4.).(Wang et al., 2015).

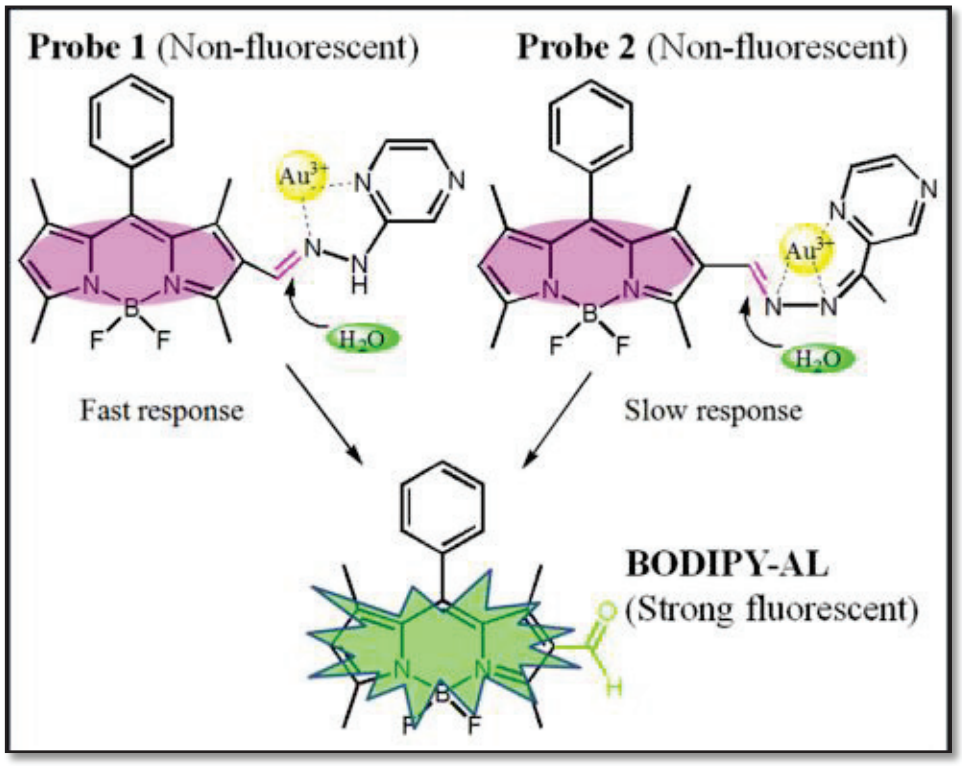

Figure 2.4. A high-performance Schiff-base fluorescent probe for monitoring Au^{+3} in zebrafish based on BODIPY.(Source: Wang et al., 2015).

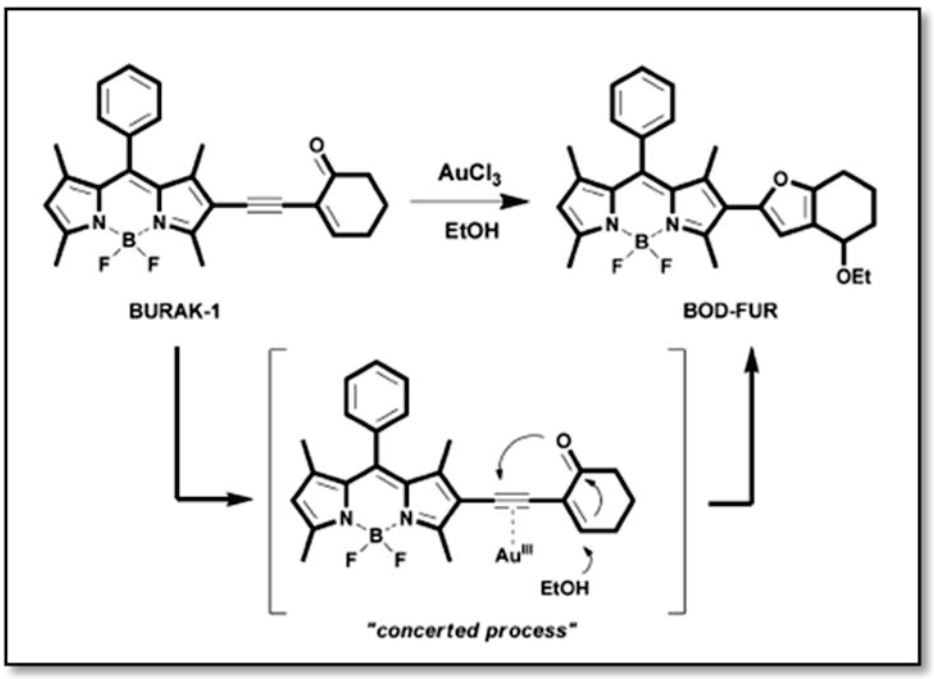

Figure 2.5. A Ratiometric Fluorescent Probe for Gold and Mercury Ions (Source: Emrullahoglu et al., 2015).

Emrullahoglu et al. (2015) reported on a fluorescent probe that displays a ratiometric fluorescence response toward gold and mercury ions. BODIPY dye was derived with an enynone structure. In the presence of a gold ion, the sensor structure has evolved as another BODIPY derivative by using the gold-catalyzed intramolecular cyclization method. In the presence of a gold ion, the long wavelength of the dye (orange) was developed through a ratiometric method as a probe by shifting to the shorter wavelength. This probe has a dual character and can detect both gold and mercury ions with a low detection limit. (Figure 2.5.)

A year later, Emrullahoglu (2016) reported another BODIPY-based fluorescent probe for the ratiometric detection of gold ions with the utilization of Z-enynol as the reactive unit. In this study, BODIPY dye was derived with a reactive Z-enynol motif. In the presence of gold catalysis, Z-enynols can be effectively cyclized to the corresponding furan derivatives. Using a non-reversible, intramolecular cyclization pathway triggered by gold ions, the probe displays ratiometric fluorescence behaviour. As a result, the probe demonstrates a highly specific response to gold species in the solution and has proved highly successful in imaging gold ions in living cells. (Figure 2.6.)

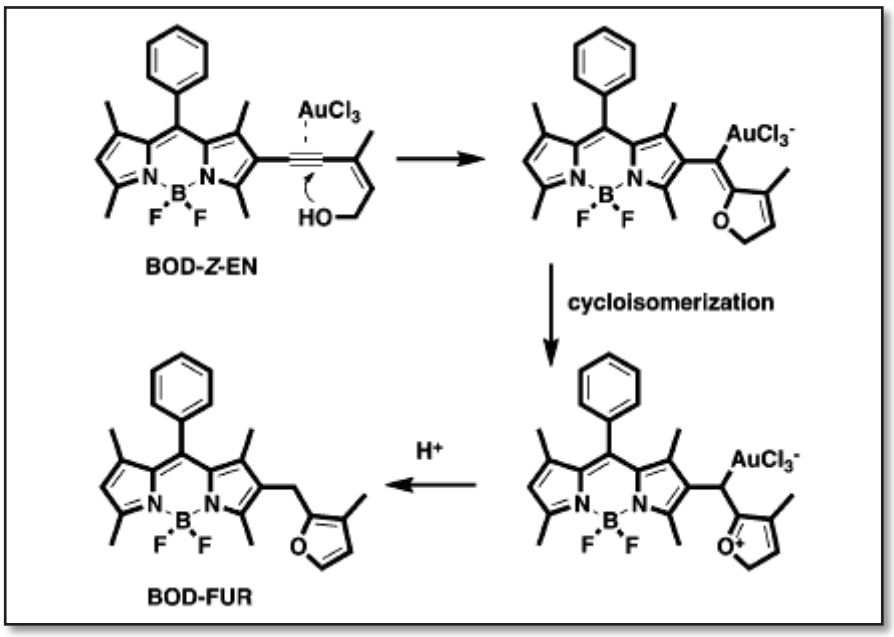

Figure 2.6. A Bodipy-based fluorescent probe for ratiometric detection of gold ions: utilization of Z-enynol as the reactive unit. (Source: Emrullahoglu et al., 2016).

2.2 "On-Off " probe for gold ion

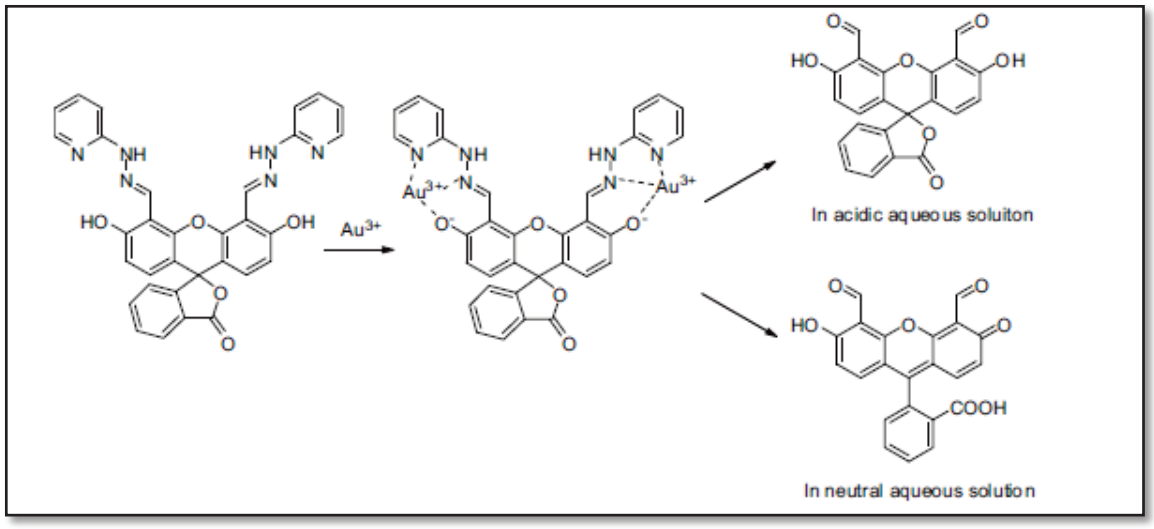

Figure 2.7. A highly sensitive and selective fluorescein-based fluorescence probe for $Au^{3+}$and its application in living cell imaging (Source: Kambam et al., 2014).

In 2014, Kambam published a report on a new fluorescein-based fluorescent probe for the detection of Au^{3+}. This probe was derived from 4,5-fluorescein dicarboxaldehyde and exhibited a highly selective and sensitive response toward gold (III) ions in an aqueous solution. It was hypothesized that the selective fluorescence response to Au^{3+} was related to non-reversible C=N bond hydrolysis induced by Au^{3+}. This probe also proved highly effective for imaging gold ions in living cells (Figure 2.7.)

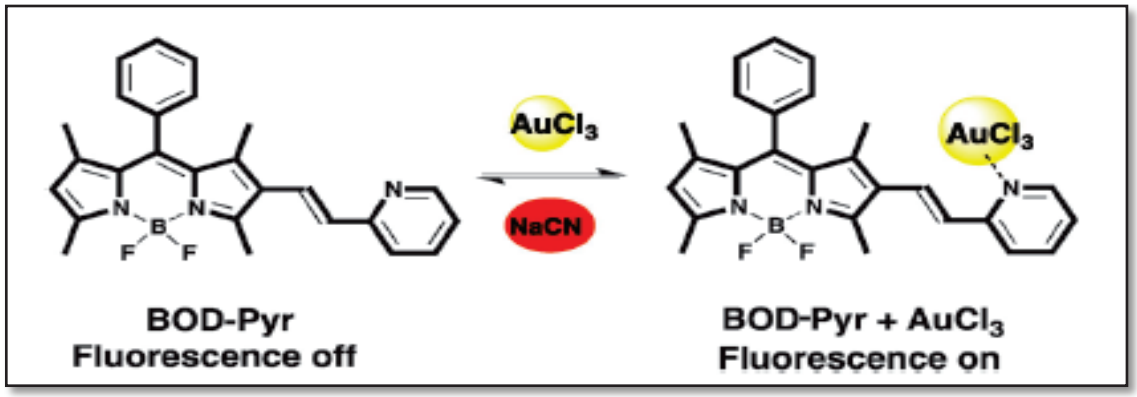

Figure 2.8. A BODIPY/pyridine conjugate for reversible fluorescence detection of gold(III) ions (Source : Emrullahoglu et al., 2015).

Emrullahoglu et al. (2015) designed and synthesized a new ‘‘turn-on’’ type of fluorescent probe based on a BODIPY–pyridine conjugate. The synthesized BOD-pyr structure is one of the rare fluorescent probe types that works reversibly against gold species. The detection-sensing of BOD-Pyr is based on the selective binding of gold ions to the pyridyl nitrogen atom recognized by a significant change in the emission intensity. The probe shows high selectivity toward Au(III) ions and also responds to changes in pH within the acidic pH range. (Figure 2.8.)

A year later, Emrullahoglu et al. (2015) reported on a turn-on type chemodosimeter based on a fluorescein scaffold for the selective detection of gold(III) ions. In this study, a fluorescein derivative was used as a fluorophore, and a reactive alkyne unit was used as a receptor. The probe showed high water solubility, a low detection limit, rapid response time, and applicability in imaging gold(III) ions in living cells. (Figure 2.9.).

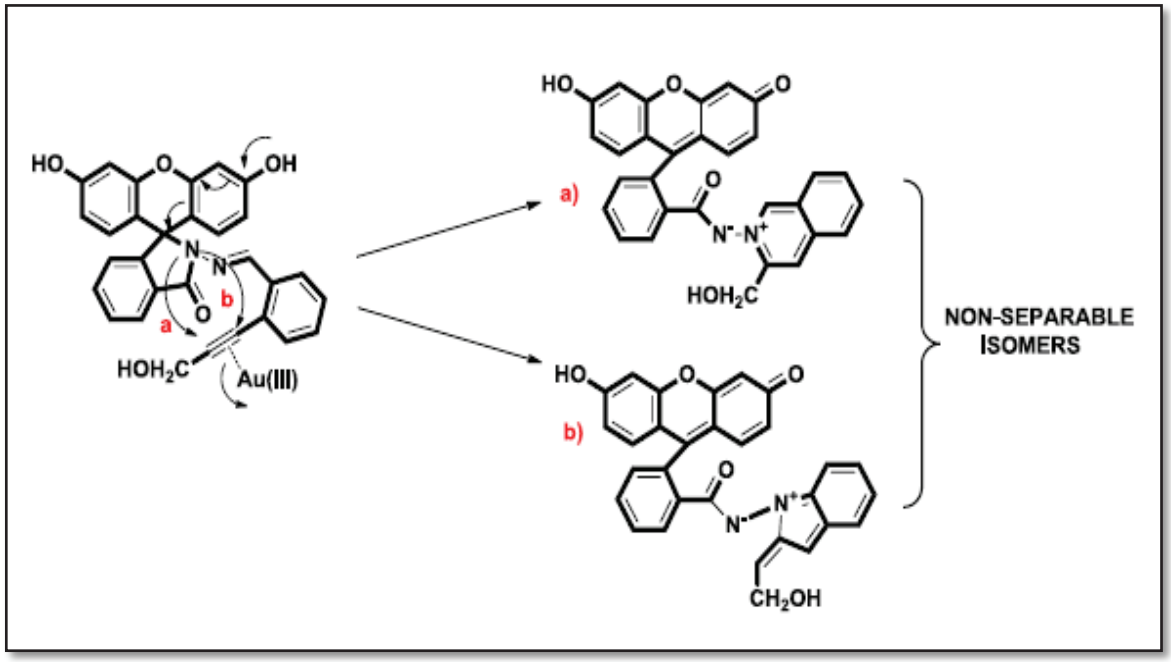

Figure 2.9. A fluorescein-based chemodosimeter for selective gold (III) ion monitoring in aqueous media and living systems (Source: Emrullahoglu et al., 2016).

In 2017, Srisuratsiri published a report on a reversible rhodamine-alkyneAu^{3+}-selective chemosensor. A rhodamine-based fluorescent chemosensor was derived with reactive alkyne moiety. Generally, reactive moiety mostly reacts with gold ion non-reversibly. However, in this study, reactive alkyne moiety reacts with in a reversible

pathway. The probe has higher selectivity and sensitivity toward gold (III) ion.The chemosensor is membrane permeable and capable of monitoring Au^{3+} in cultured HeLa cells. (Figure 2.10.)

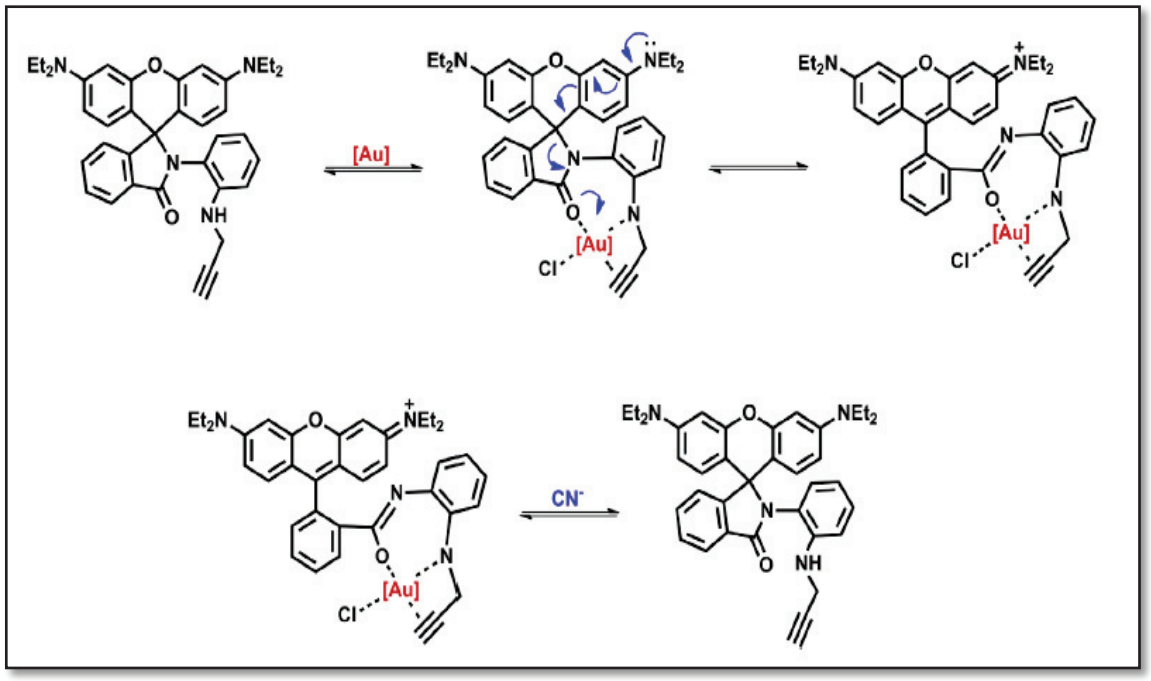

Figure 2.10. Reversible rhodamine-alkyne Au3+-selective chemosensor and its bioimaging application (Source: Srisuratsiri et al., 2017).

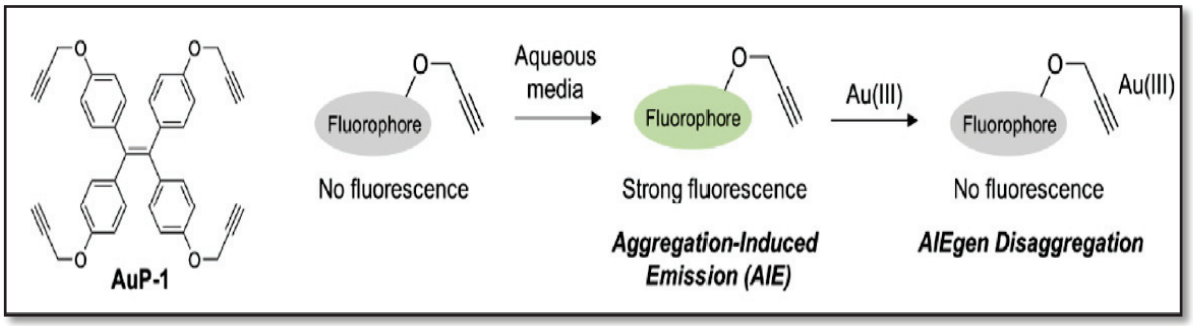

Figure 2.11. A highly sensitive and fast responsive fluorescent probe for the detection of gold (III) ions based on the AIEgen disaggregation(Source: Kim et al., 2018).

In 2018, Kim reported that a fluorescent probe for gold ions, Au(III), was developed based on Au(III)-induced disaggregation of AIEgen for the first time. Unlike other probe mechanisms, the AIEgen disaggregation method was used in this study. This probe is based on the propellant tetraphenylethylene (TPE), which is a non-emissive and

dispersant in the aggregated form, stimulated by free rotation, non-radial degradation of fluorescence, which limits the activation of intermolecular rotation. In this research, the probe showed high sensitivity, rapid response time, and high selectivity. It also detected Au^{+3} ions in the cell and paper-based strip was successfully realized. (Figure 2.11.)

CHAPTER 3

EXPERIMENTAL STUDY

3.1. General

All reagents were purchased from commercial suppliers (Aldrich and Merck) and used without further purification. ^{1}H NMR and ^{13}C NMR were measured on a Varian VNMRJ 400 Nuclear Magnetic Resonance Spectrometer. UV absorption spectra were obtained on Shimadzu UV-2550 Spectrophotometer. Fluorescence emission spectra were obtained using Varian Cary Eclipse Fluorescence Spectrophotometer. Cell imaging was performed with a Zeiss Axio fluorescence microscope. Samples were contained in 10.0 mm path length quartz cuvettes (2.0 mL volume). Upon excitation at 460 nm, the emission spectra were integrated over the range 480 nm to 700 nm (Both excitation and emission slit width 5 nm / 5 nm). pH was recorded by HI-8014 instrument (HANNA). All measurements were conducted at least in triplicate

3.2. Determination of quantum yields

Fluorescence quantum yields of synthesized probe molecules were determined by using optically matching solutions of mostly Rhodamine 6G (ΦF=0.95 in water) as a standard (Brouwer, 2011). The quantum yield was calculated according to the equation.

$$\Phi_{F(X)} = \Phi_{F(S)} (A_S F_X / A_X F_S) (n_X / n_S)^2$$

Where Φ_F is the fluorescence quantum yield, A is the absorbance at the excitation wavelength, F is the area under the corrected emission curve, and n is the refractive index of the solvents used. Subscripts S and X refer to the standard and to the unknown, respectively.

3.3. Synthesis of Probe Molecule

The synthesis pathway for BOD-EN was shown in Figure 3.1. BOD , BOD-I and BOD-AC were synthesized using the literature procedure. BOD-AC was converted to BOD-EN form by using the well-known Sonogashira coupling reaction.

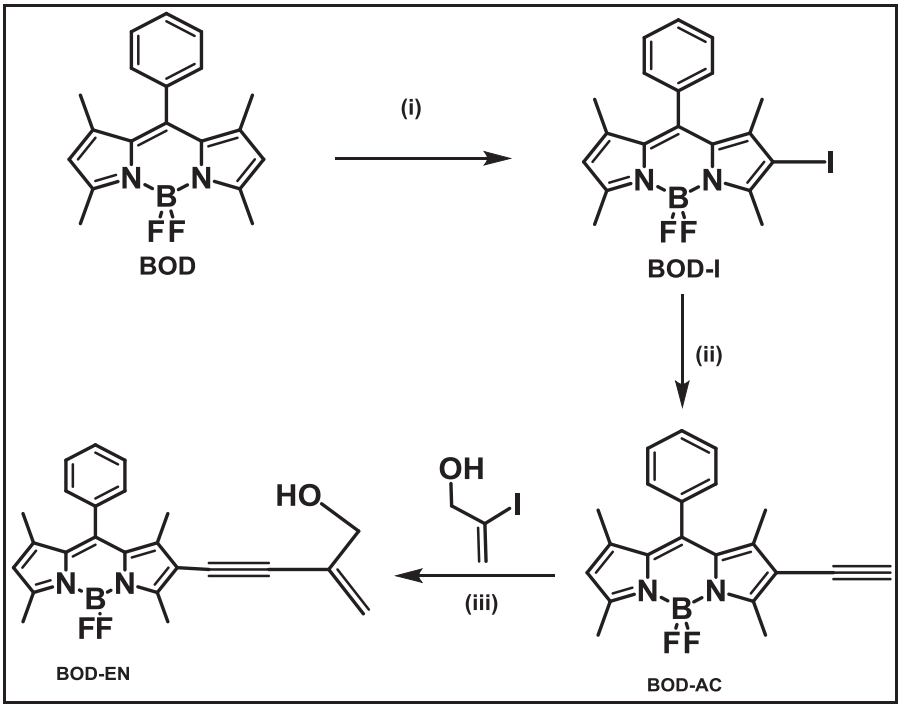

Figure 3.1. Synthesis pathway of BOD-EN. (i) 1 equiv. NIS, DCM, RT, overnight (ii) 1)TMS-acetylene, $Pd(PPh_3)_2Cl_2$, CuI, THF, DIPEA, 50°C 2) K_2CO_3, MeOH, (iii) $PdCl_2(PPh_3)_2$,CuI, THF, DIPEA, 50°C.

3.3.1. Synthesis of BOD

BODIPY was synthesized using the procedure in the literature (Sauer et al., 2012). Benzaldehyde (200 µL, 2 mmol) and several drops of trifluoroacetic acid were added to a solution of 2,4-dimethylpyrrole (500 µL, 5 mmol) in 25 mL of dry THF under an argon atmosphere. The solution was stirred at room temperature overnight. After overnight stirring, 2,3-Dichloro-5,6-dicyano-p-benzoquinone (DDQ; 455 mg, 2 mmol) was dissolved into 25 mL of dry THF and was added to the mixture drop by drop. The mixture was stirred for 4 hours. After 4 hours, triethylamine (12 mL) was added, and the mixture

was stirred for 30 minutes. Lastly, $BF_3.Et_2O$ was added to the mixture, then the mixture was again stirred at room temperature overnight. After completion of the reaction, the solvent was removed under reduced pressure. The mixture was extracted with DCM, dried over $MgSO_4$ and concentrated under reduced pressure. The product was purified by column chromatography with a 40% yield (232 mg) as an orange solid..^{1}H NMR (400 MHz, $CDCl_3$) δ: 7.49-7.47 (m, 3H), 7.28-7.26 (m, 2H), 5.98 (s, 2H), 2.55 (s, 6H), 1.37 (s, 6H). ^{13}C NMR (100 MHz, $CDCl_3$) δ: 155.4, 143.2,141.7, 135.0, 129.1, 128.9, 127.9, 121.29, 14.59, 14.34.

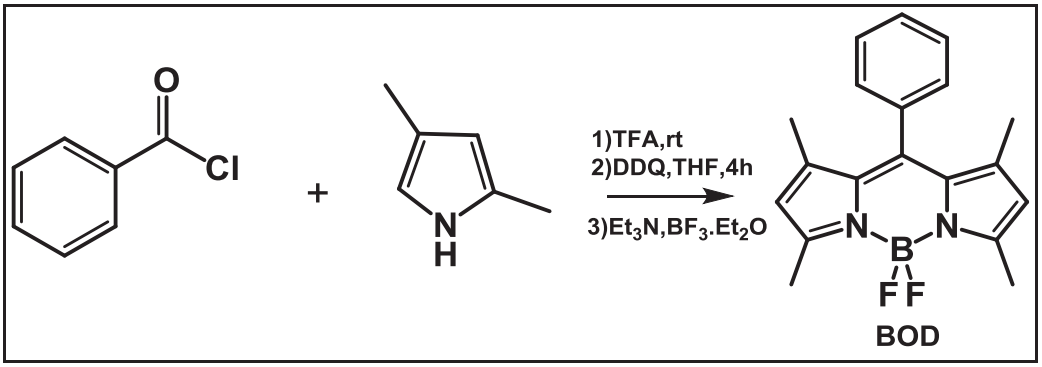

Figure 3.2. Synthesis of Bodipy

3.3.2. Synthesis of BOD-I

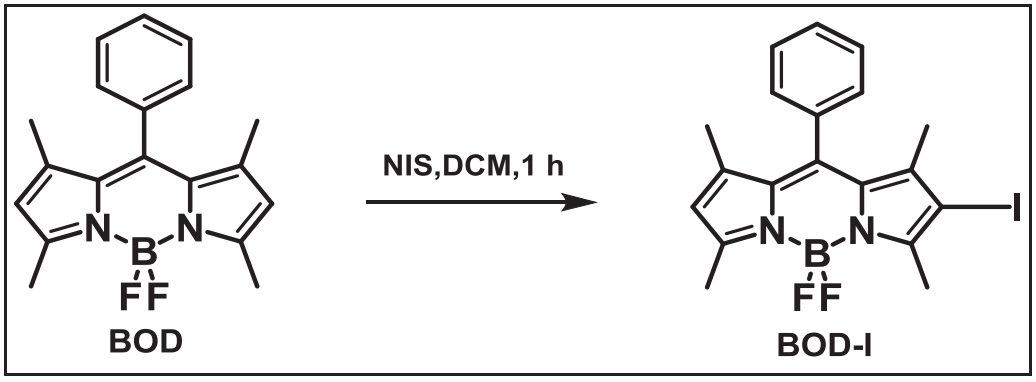

Figure 3.3. Synthesis of Bod-I

BODIPY (100 mg, 0,3 mmol) was dissolved in 25 mL of dry DCM. Then, NIS (N-iodosuccinimide) (70 mg, 0.3 mmol) in 10 mL of DCM was added at 10^0C. The mixture was stirred for 1 hour. After 1 hour, the solvent in the mixture was evaporated

under reduced pressure. The product was purified by column chromatography as an orange solid.^{1}H NMR (400 MHz, $CDCl_3$): δ: 7.51−7.48 (m, 3H), 7.27−7.25 (m, 2H), 6.04 (s, 1H), 2.63 (s, 3H), 2.57 (s, 3H), 1.38 (s, 6H).^{13}C NMR (100 MHz, $CDCl_3$): δ: 157.9, 154.7, 145.3,143.4, 141.7, 135.0, 132.0, 131.1, 129.8, 129.5, 129.4, 128.0, 122.5, 84.4,16.8, 16.0, 14.9, 14.7.

3.3.3. Synthesis of BOD-AC

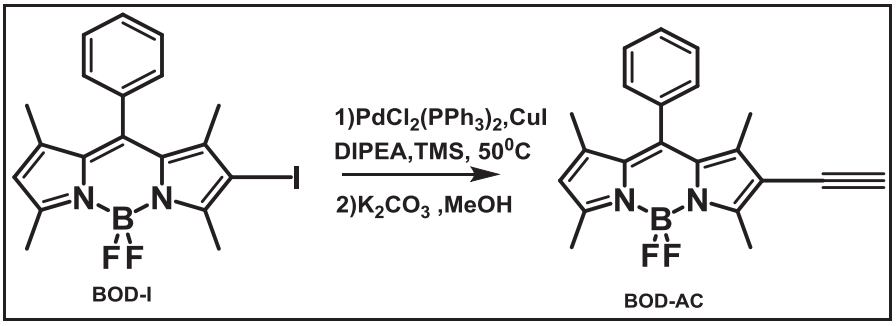

Figure 3.4. Synthesis of Bod-AC

Trimethylsilylacetylene (85 µL, 0,6 mmol) in dry THF was added to a solution of BODIPY-I (115 mg, 0.25 mmol) and the mixture was degassed. While the mixture was degassing, $PdCl_2(PPh_3)_2$ (22 mg, 0.1 equiv.), CuI (8 mg, 0.2 equiv.) and 3.9 mL of DIPEA were added. The reaction was degassed for 30 minutes. The mixture was stirred overnight at 50^{0}C. After overnight stirring, the solvent was evaporated under reduced pressure. The mixture was extracted with DCM, dried over $MgSO_4$ and concentrated under reduced pressure. The product was purified by column chromatography to yield a dark orange solid. To a solution of BODIPY-TMS, 20 mL of MeOH and K_2CO_3 (30 mg, 0,2 mmol) were added. The reaction was controlled by TLC. After completion of the reaction, the mixture was extracted with DCM, dried over $MgSO_4$ and concentrated. The product was purified by column chromatography to yield BOD-AC as a greenish orange solid. (70 mg, 60% yield).^{1}H NMR (400 MHz, $CDCl_3$): δ 7.52 7.49 (m, 3H), 7.28 7.25(m, 2H), 6.04 (s, 1H), 3.28 (s, 1H), 2.64 (s, 3H), 2.57 (s, 3H), 1.44(s, 3H), 1.39 (s, 3H). ^{13}C NMR (100 MHz, $CDCl_3$): δ 158.3, 156.7,145.2, 143.8, 142.5, 135.4, 134.7, 132.8, 130.0, 129.4, 128.0, 125.2, 122.5,114.1, 83.5, 76.6, 14.9, 14.7, 13.5, 13.1.

3.3.4. Synthesis of 2-iodoprop-2 en1-ol

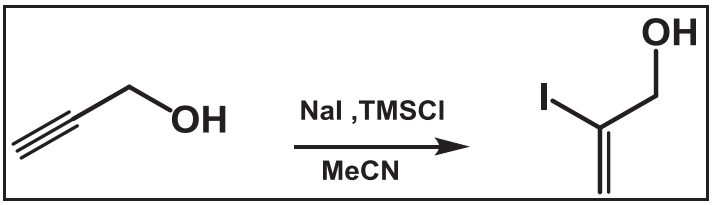

Figure 3.5. Synthesis of reactive motif

A solution of sodium iodide (1.2 g, 8,6 mmol) was dissolved in acetonitrile (10 ml) and water (0,1 ml). Chlorotrimethylsilane (TMSCl; 1 ml, 8,6 mmol) was added at room temperature.After 10 minutes of stirring, propargyl alcohol (0,25 ml, 4.2 mmol) was added to the mixture and it was stirred for 90 minutes. Then, the reaction mixture was diluted with 25 ml of water and 25 ml of 5% aqueous $Na_2S_2O_3$. The aqueous phase extracted the mixture with DCM; it was then dried over $MgSO_4$. The crude product was purified by column chromatography with 58% yield as a brown oil. ^{1}H NMR (400 MHz, $CDCl_3$): H 2.00 (bs, 1H), 4.18 (d, J = 5.7 Hz, 1.3H), 4.28 (d, J = 6.2 Hz, 0.7H), 5.86 (dt, J = 2.1,1.1 Hz, 1H), 6.39 (q, J = 1.5 Hz, 1H).^{13}C NMR (100 MHz, $CDCl_3$): 124.6, 110.6 ,71.2.

3.3.5. Synthesis of BOD-EN

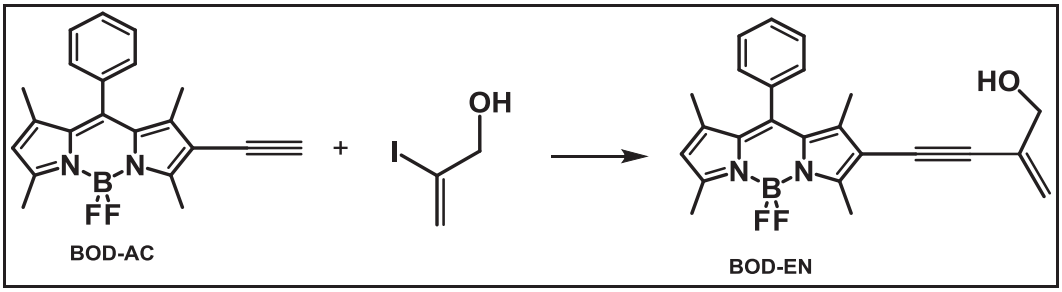

Figure 3.6. Synthesis of BOD-EN

To a mixture of BOD-AC (70 mg, 0.2 mmol) and 2-iodoprop-2 en1-ol (73,5 mg, 0.4 mmol) in THF(10 mL), $PdCl_2(PPh_3)_2$ (14.02 mg, 0.1 equiv.) and CuI (7,6 mg, 0.2equiv.) were added. The resulting mixture was degassed for 10 minutes and 5,8 mL of DIPA was

added. The reaction mixture stirred overnight at 50°C. After completion of the reaction, the solvent was removed under vacuum, and the resulting residue was extracted with DCM. The organic layer was dried over MgSO4, filtered and concentrated. The resultant residue was purified by column chromatography (2:1(Hexane:Ethyl acetate)) to afford BOD-EN as a red solid ^{1}H NMR (400 MHz, $CDCI_3$) δ= 7.51 – 7.48 (m, 2H), 7.28 – 7.25 (m, 3H), 6.03 (s, 1H), 5.54 – 5.50 (m, 1H), 5.47 (dd, *J* = 2.5, 1.2 Hz, 1H), 4.19 (s, 2H), 2.63 (s, 3H), 2.57 (s, 3H), 1.43 (s, 3H), 1.39 (s, 3H). ^{13}C NMR (100 MHz, $CDCI_3$) δ= 157.9, 156.2, 144.9, 142.7, 142.1, 134.6, 131.3, 129.2, 129.1, 127.8, 122.2, 119.3, 93.3, 83.7, 65.5, 31.9, 29.7, 22.7, 14.8, 14.5, 14.1, 13.5, 13.1.MS HRMS (TOF-APCI): m/z Calcd. For $C_{24}H_{23}BF_2N_2O$: 404.19 $[M-H]^+$, Found: 405.195$[M-H]^+$.

3.3.6. Synthesis of BOD-FUR

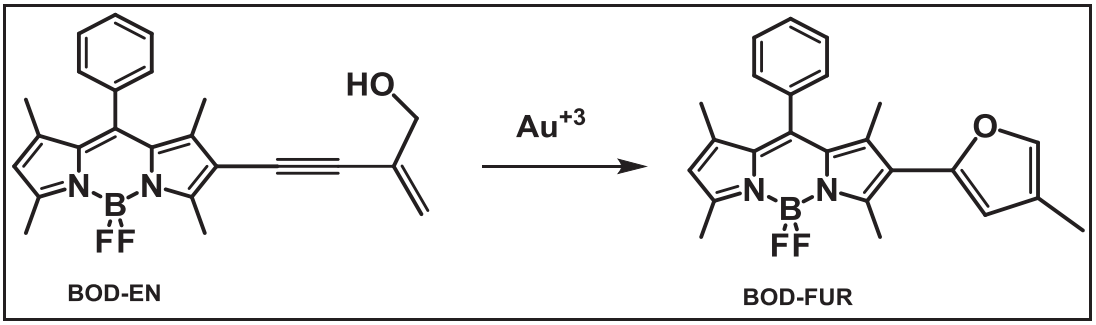

Figure 3.7. Synthesis of BOD-FUR

To a solution of BOD-EN (40,5 mg, 0.1 mmol) in a PBS/ethanol solution (10 mL,(7/3 (v/v)) 1 equivalent of $AuCl_3$ was added and the reaction mixture was stirred for 2 hours. The resulting solution was extracted with DCM and dried over MgSO4. After the evaporation of solvent, the resultant residue was purified by column chromatography.^{1}H NMR (400 MHz, $CDCI_3$) δ= 7.50 – 7.48 (m, 3H), 7.31 – 7.28 (m, 2H), 7.21 – 7.19 (m, 1H), 6.10 – 6.09 (m, 1H), 6.01 (s, 1H), 2.68 (s, 3H), 2.57 (s, 3H), 2.05 (d, J = 1.1 Hz, 3H), 1.43 (s, 3H), 1.38 (s, 3H). ^{13}C NMR (101 MHz, cdcl3) δ 156.50, 154.36 , 148.25, 143.92 , 142.19 , 139.02, 138.58 , 135.17 , 132.08 , 130.95 , 129.26 , 128.16 , 123.40 , 121.83 , 121.20 , 111.60 , 14.70 , 14.05 , 12.97 , 9.95 .MS HRMS (TOF-APCI): m/z Calcd. for$C_{24}H_{23}BF_2N_2O$: 404.19498 $[M-H]^+$, Found: 405.3590 $[M-H]^+$.

3.4. General Mechanism of Reaction

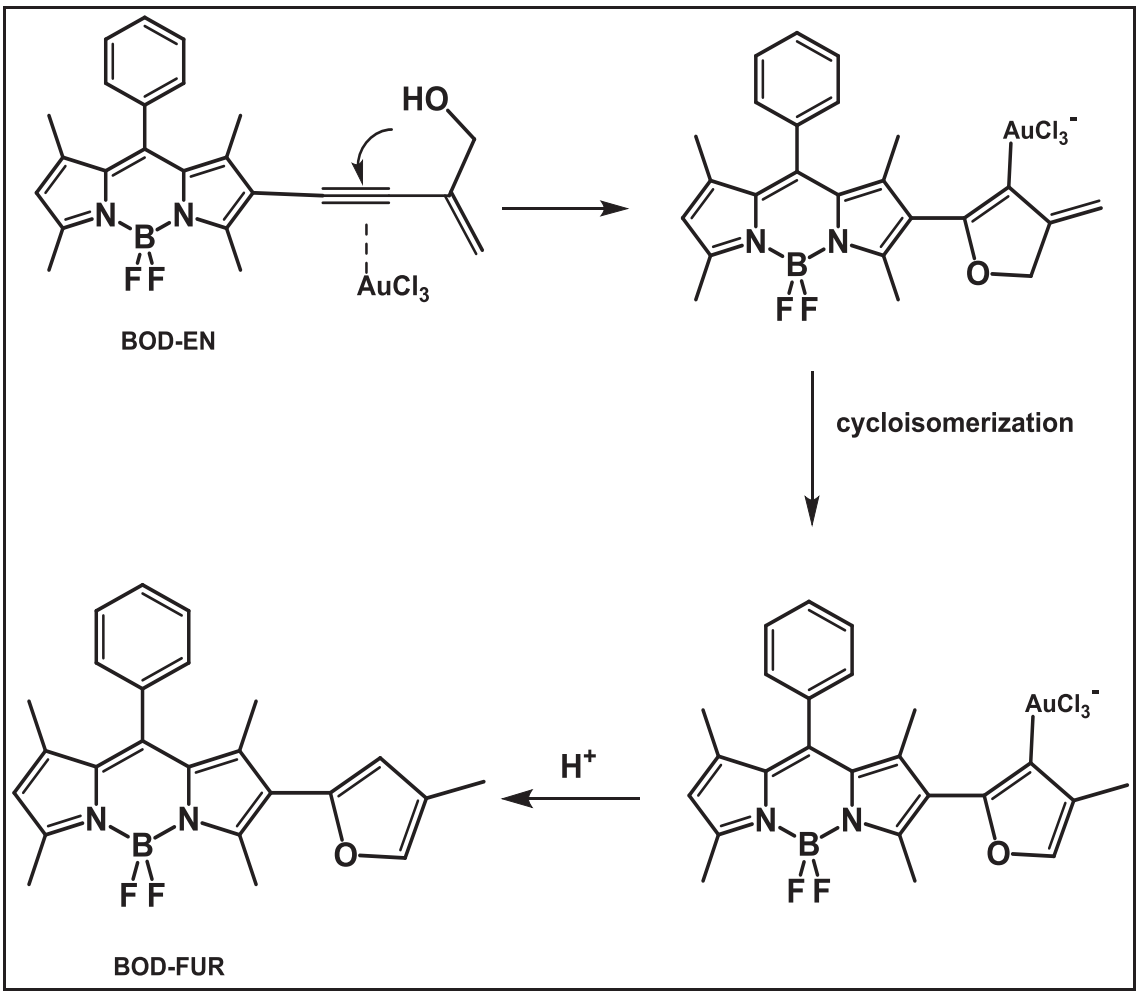

Figure 3.8. Mechanism for gold ion catalysed intramolecular cyclisation.

According to reports in the literature, gold ions activate triple bonding. It is also reported that enynol structure enhances the electrophilicity of alkyne for $AuCl_3$ (Liu et al., 2005). Gold ions activate the triple bond because of pi-conjugation. The hydroxyl group makes a nucleophilic attack and intramolecular exo-dig cyclisation of the hydroxyl group causes the triple bond. The next step, the BODIPY derivative, is formed by cycloisomerization. In the last step, the BODIPY derivative is formed by means of the protonolysis pathway, yielding the BODIPY-FURAN structure. (Figure 3.

CHAPTER 4

RESULTS AND DISCUSSION

4.1. Spectroscopic Results of BOD-EN

In this study, a new gold ion sensor based on a BODIPY derived with iodo-allyl alcohol was developed. It is known from the literature that the enynol motif can cyclize to furan derivatives in the presence of gold ions. Based on previous studies in our laboratory, we had knowledge of intramolecular cyclization triggered by gold ions. Based on these conditions, BOD-EN was designed and synthesized.

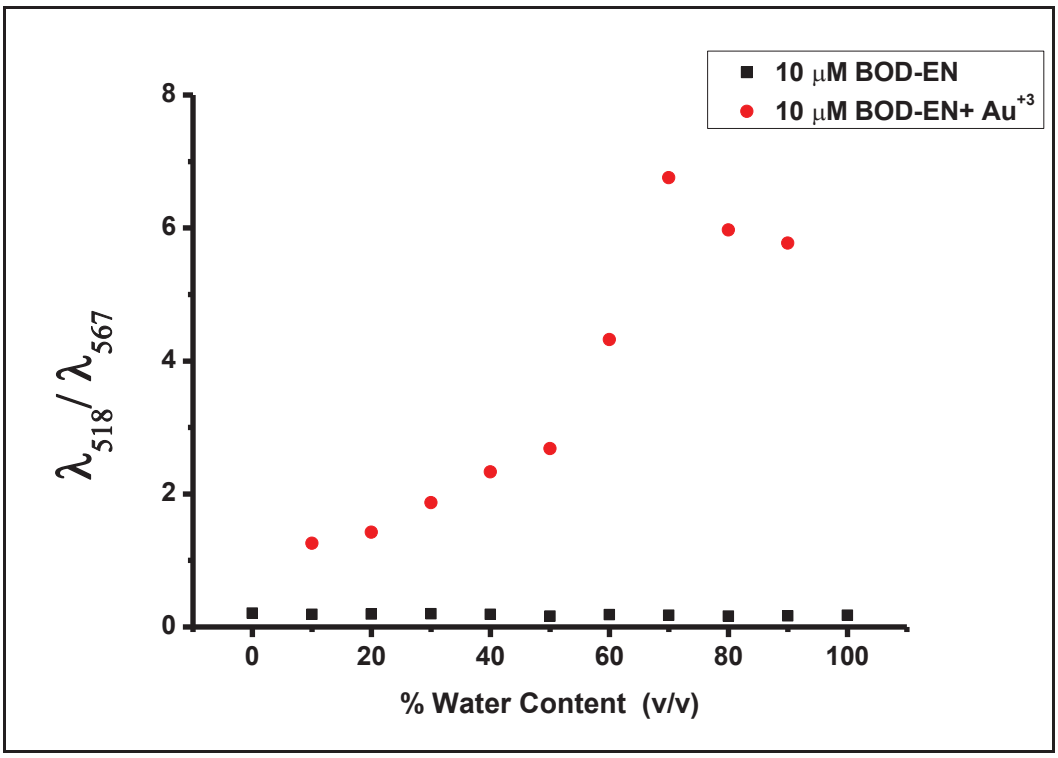

Figure 4.1. Effect of fraction of water on the interaction of BOD-EN (10 μM) with Au^{3+} (100μM, 10 equiv.) in 0.01M PBS buffer, pH 7.0/EtOH (v/v, 7:3) (λ_{ex}: 460 nm,emission wavelengths: λ_{518}/ λ_{567} at 25°C).

The investigation began with the evaluation of the optical behaviour of BOD-EN in different solvents, such as phosphate/EtOH, CH_3CN/HEPES buffer solvent. The highest florescent ıntensity was observed in a 0.01 M PBS/EtOH solvent system, with visibility to the naked eye.In the following step, different ratios of the PBS-EtOH system were examined. The best result was obtained in the 0.01 M PBS/EtOH (v/v, 7:3)H (v/v, 7:3). (Figure 4.1).

The effect of the fraction of pH on the interaction of BOD-EN was investigated for Au^{+3}. The probe has a fluorescent intensity between the pH values of 2–10 pH; from 10 to 12, the probe has a low fluorescence intensity. This shows that the probe did not work well in basic media.It can also be shown that the probe provides better results in acidic than in basic media. As shown in Figure 4.2, the highest fluorescence intensity was observed data pH of 7. The highest value of the probe at pH 7 indicates that it fulfils a basic requirement for cell bioimaging. (Figure 4.2).

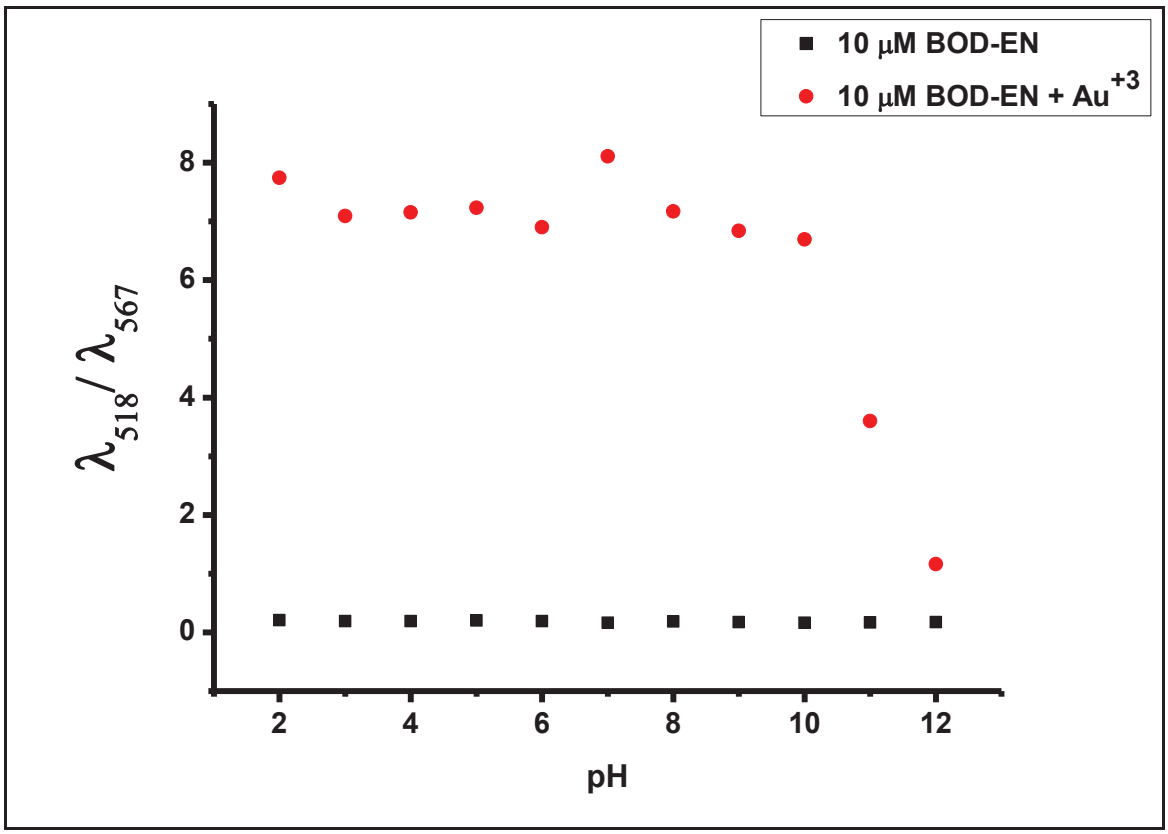

Figure 4.2. Effect of fraction of pH on the interaction of BOD-EN (10 μM) with Au^{3+} (100μM, 10 equiv.) in 0.01M PBS buffer, pH/EtOH (v/v, 7:3) (λ_{ex}: 460 nm,emission wavelengths: λ_{518}/ λ_{567}at 25°C).

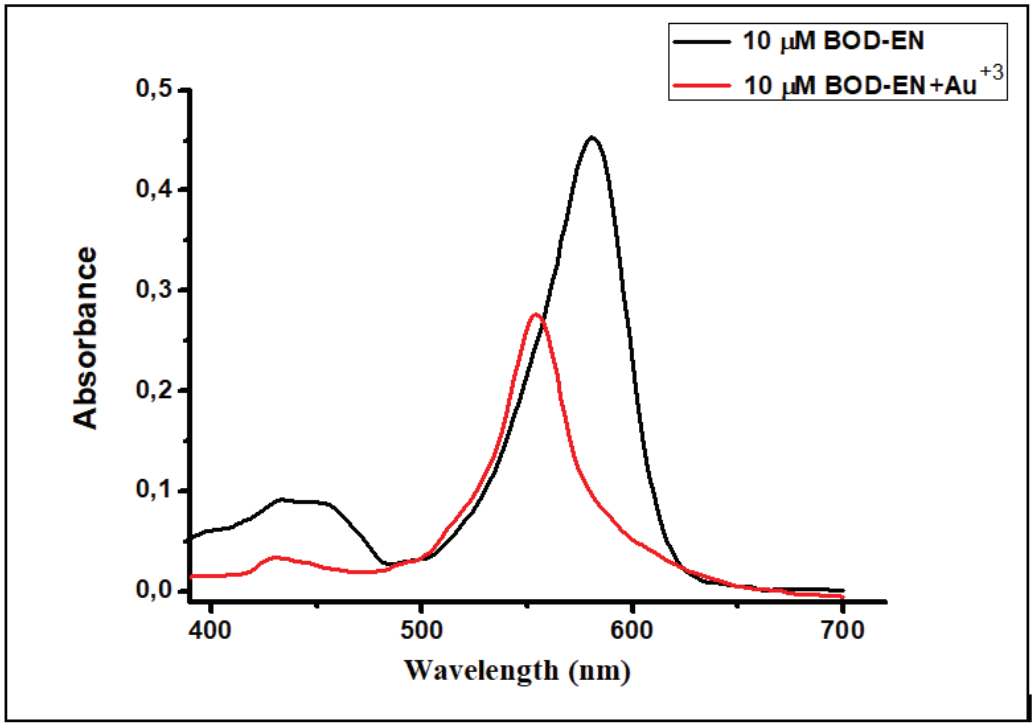

Figure 4.3. Absorbance spectra of BOD-EN (10 μM) in the absence and presence of 20 equiv. (200 μM) of Au^{3+} in 0.01 M PBS buffer/EtOH (pH 7.0, v/v,7:3) (λ_{ex}: 460 nm at 25ºC).

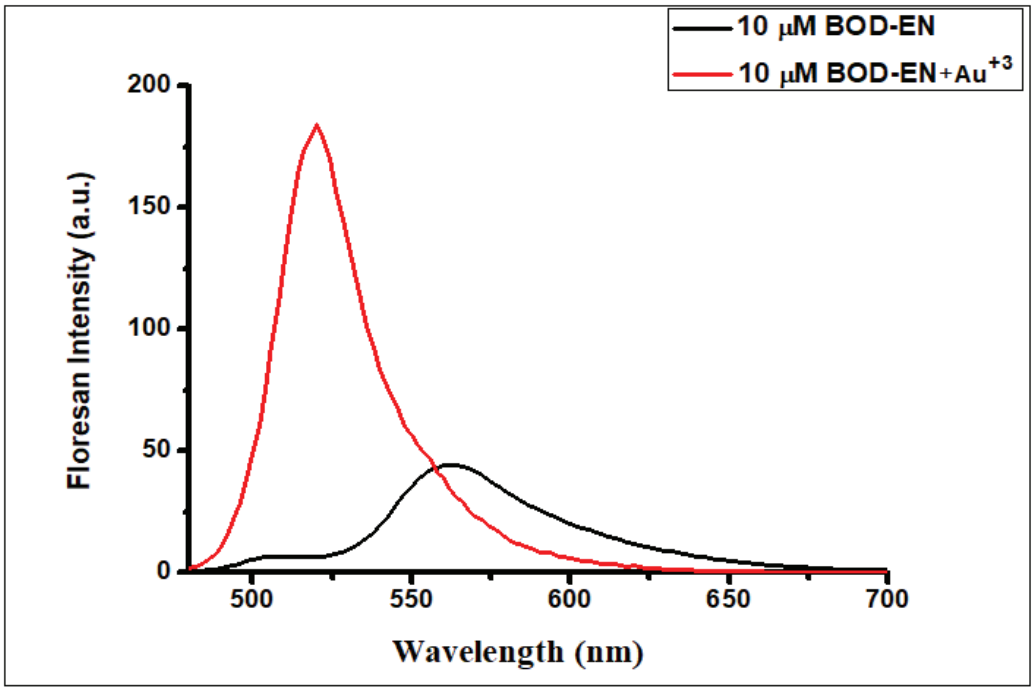

Figure 4.4. Fluorescence spectra of BOD-EN (10 μM) in the absence and presence of 20 equiv. (200 μM) of Au^{3+} in 0.01 M PBS buffer/EtOH (pH 7.0, v/v,7:3) (λ_{ex}: 460 nm at 25ºC).

In the following step, the optical behaviour of the probe in response to the presence of Au^{+3} was examined. As shown in Figure 4.3, BOD-EN displayed a single absorption band at 581 nm. In the presence of Au^{+3}, the absorption band decreased to 553 nm. As shown in Figure 4.4, with the addition of Au^{+3}, the emission band at 567 nm diminished, and a new emission band with a maximum at 518 nm increased. The solution colour changed from orange to green, facilitating direct observation with the naked eye.

The investigations were continued with the systematic titration of gold ions. When the concentration of gold ions increased, the intensity of fluorescence emission at 518 nm increased proportionally. After the addition of 6 equivalents of Au^{3+} ions, the system became saturated, and the fluorescence intensity became stabilized. (Figure 4.5).

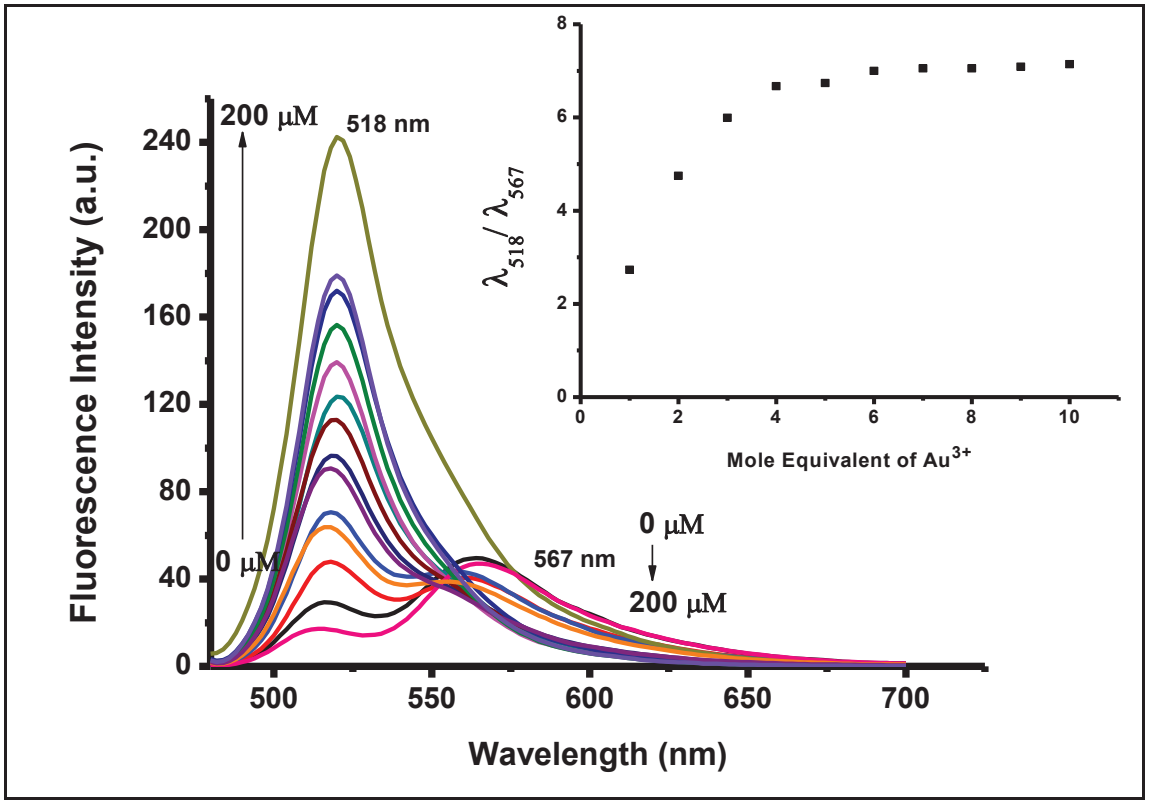

Figure 4.5. Fluorescence spectra of BOD-EN (10 μM) in the presence of increasing amount of Au^{3+} (0-100 μM) 0.01 M PBS buffer/EtOH (pH 7.0, v/v,7:3).Inset: Calibration curve. (λ_{ex}: 460 nm at 25°C).

The detection limit was calculated based on fluorescence titration. To determine the detection limit, the emission intensity of BOD-EN (10μM) without Au^{3+} was measured 10 times, and the standard deviation of blank measurements was determined. Under the present conditions, a good linear relationship between fluorescence intensity

and Au^{3+} concentration could be obtained in the range of 0.1–0.9 μM (R = 0.9815)(Figure 4.6). The detection limit is then calculated with the equation: detection limit = 3σbi/m, where σbi is the Standard deviation of blank measurements, and m is the slope between intensity and sample concentration. The detection limit was measured to be 358 nM at S/N=3.

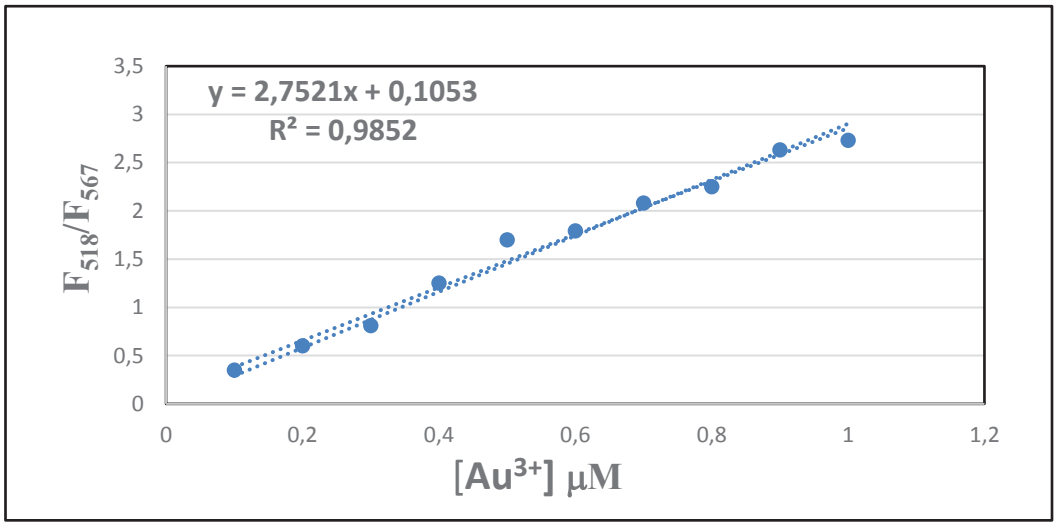

Figure 4.6. Fluorescence changes of **BOD-EN** (10.0 μM) upon addition of Au^{3+} (0. 1 to 0.9 μM, 0.01 to 0.09 equiv.) in 0.01M PBS buffer, pH 7.0/EtOH (v/v, 7:3) (λ_{ex}:460 nm, emission wavelengths: λ_{518}/ λ_{567}at 25ºC).

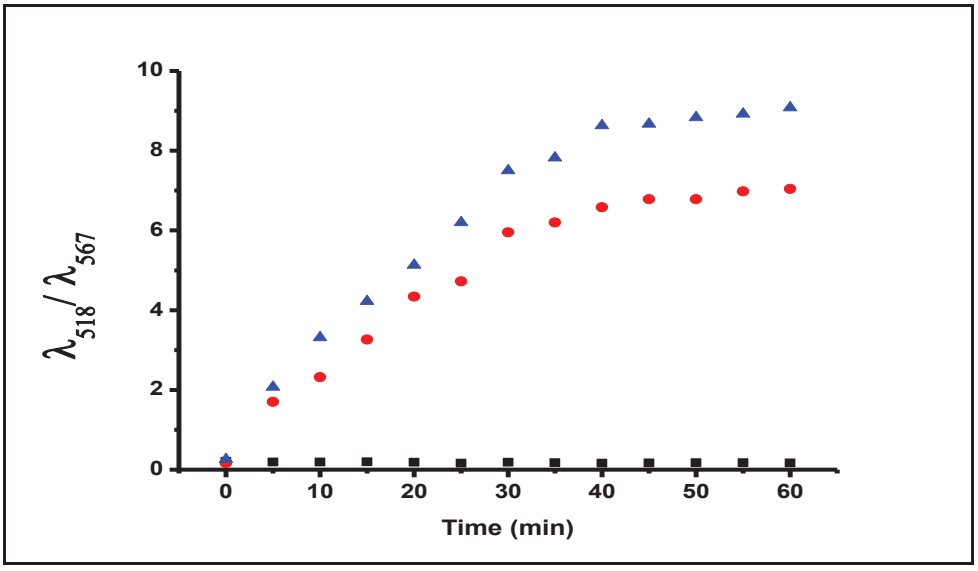

Figure 4.7. Reaction time profiles of BOD-EN (10 μM) in the absence (■) or presence of Au^{3+}[10 (●), 30(▲) μM.]. The fluorescence intensities at 518 nm and 567 nm were continuously monitored at time intervals in 0.01 M PBS buffer/EtOH (pH 7.0, v/v, 7:3) (λ_{ex}: 460 nm,emission wavelengths: λ_{518}/ λ_{567} at 25 ºC).

The reaction-time studies indicate that the maximal emission ratio was reached within 40 min. Thus, an assay period of 40 min was chosen for the evaluation of the sensitivity of the probe and its sensitivity to Au^{+3}. (Figure 4.7.)

Investigation was continued for fluorescence intensity changes of the probe upon adding other metal ions such as Pb^{+2}, Zn^{+2}, Ba^{+2},Ca^{+2}, Cd^{+2}, Co^{+2}, Cr^{+2}, Cu^{+2}, Fe^{+3}, Hg^{+2},Mg^{+2}, Ni^{+2}, K^{+1}, Na^{+1}, Li^{+1}, $Ag^{+1}$and Au^{+1}. As shown in Figure 4.8, the fluorescence of BOD-EN showed no obvious changes after the addition of metal ions except for the Au^{3+}ion. As a result, the probe has a higher selectivity for Au^{3+} than for other metal ions tested; moreover, the probe detected only the Au^{+3}ion. (Figure 4.8.)

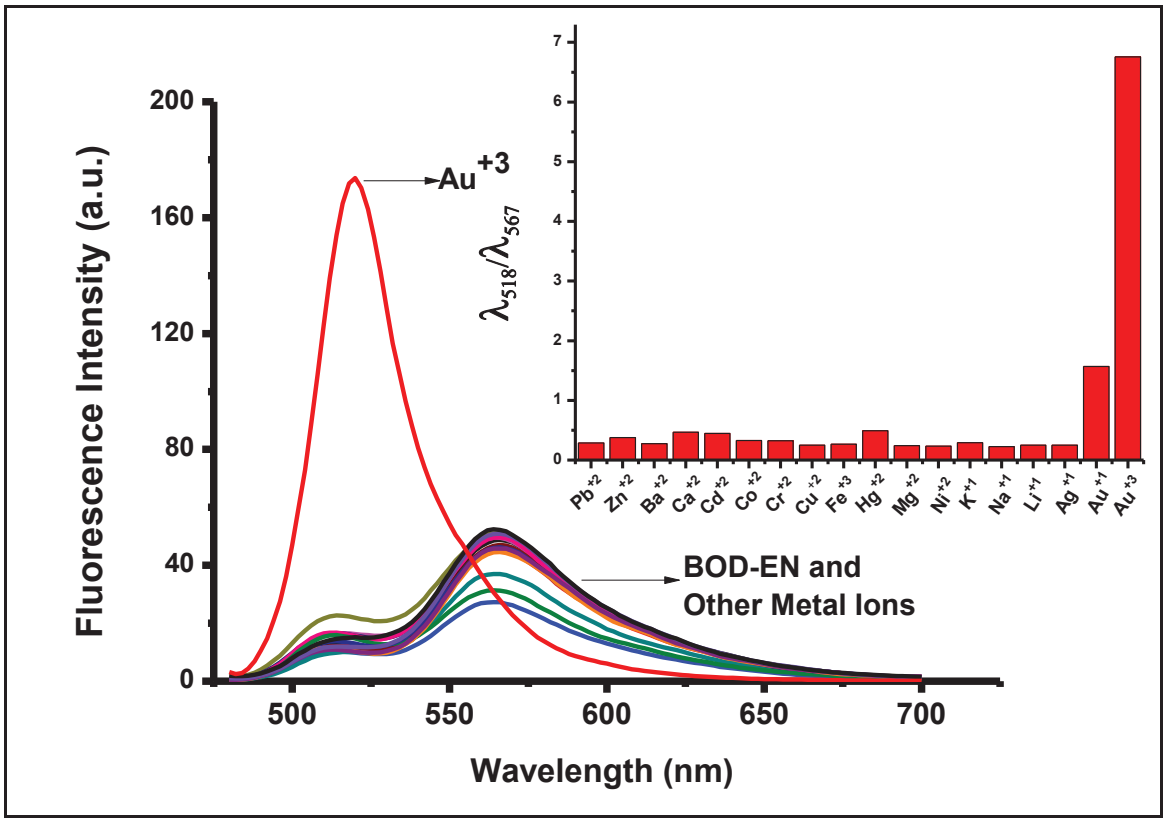

Figure 4.8. Fluorescence intensities of **BOD-EN**(10 μM), **BOD-EN**(10 μM) + Au^{3+} (100μM, 10 equiv.), **BOD-EN**(10 μM) + other metal ions (200 μM, 20 equiv.) in 0.01M PBS buffer, pH 7.0/EtOH (v/v, 7:3) (λ_{ex}: 460 nm, at 25°C). Inset: Bar graph notation.

In the last part of the measurements, as shown in Figure 4.9, bar graphs of BOD-EN toward various other metal ions in the presence of Au^{3+} were carried out to investigate the selectivity of the probe to Au^{3+} in the presence of other metal ions. Fluorescence was activated when BOD-EN and Au^{3+} ions were added to the solutions of these metal ions,

indicating that the presence of other metal ions together had little effect on the detection of Au^{+3}. As a result, the probe can effectively detect Au^{3+} ions in a mixture of other species. (Figure 4.9.)

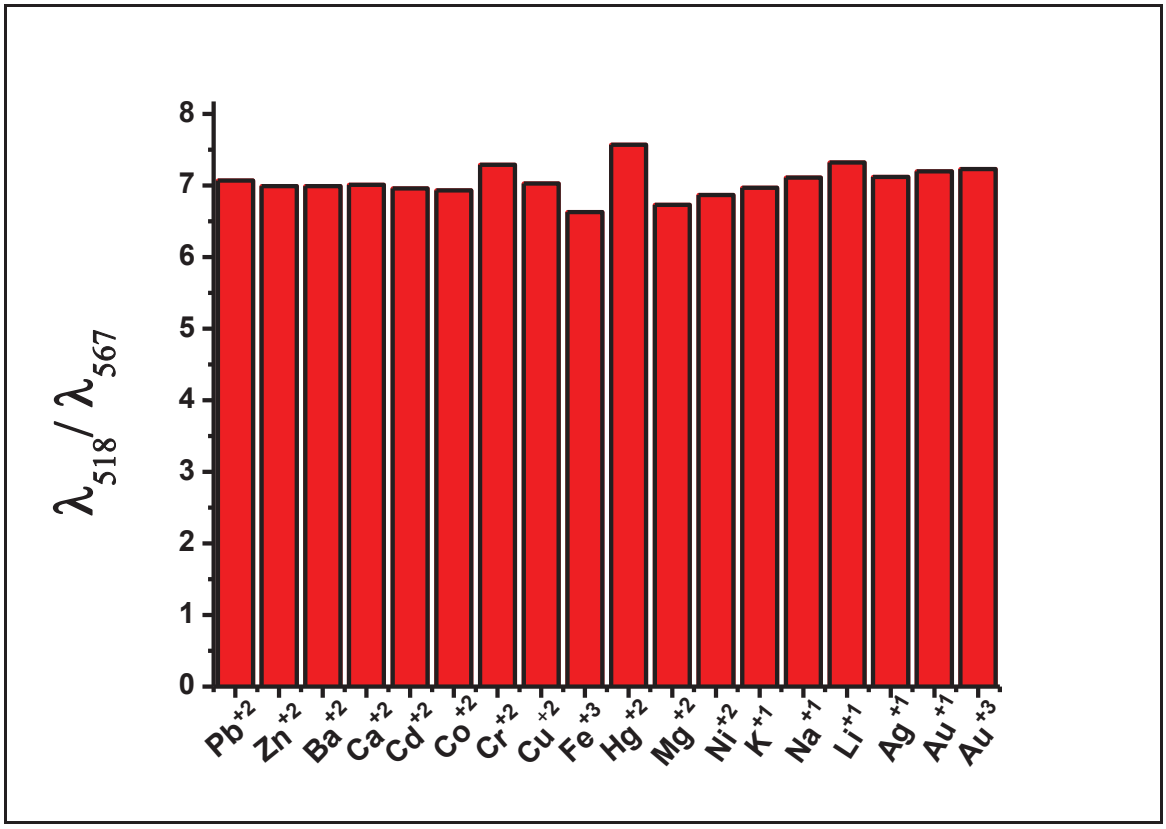

Figure 4.9. Fluorescence intensities of **BOD-EN** (10 μM) in the presence of Au^{3+} (100 μM, 10 equiv.) and 20 equiv. of other metal ions in 0.01 M PBS buffer pH 7.0/EtOH (v/v, 7:3) (λ_{ex}: 460 nm, emission wavelengths: $\lambda_{518}/\lambda_{567}$at 25°C).

4.2. Cell Imaging of BOD-EN

Because the probe provided extremely sensitive and selective responses to Au^{+3}, the potential for monitoring Au^{3+} ions in live cells was evaluated. Thus, the capability of BOD-EN for the imaging of Au^{3+} in living cells was investigated. To that end, human lung adenocarcinoma cells (A549) were incubated with the probe (10 μM) at 37°C for 20 min. In the following step, a 10 μM Au^{3+} solution was added, and the cells were incubated for 20 min. As shown in Figure 4.10a, when the cells were incubated with the BOD-EN probe (10 μM) in the culture medium for 30 min at 37°C, the cells gave off an orange

emission. Based on this result, it can be concluded that the probe is permeable to the cell. When the probe cells were treated with increasing concentrations of Au^{3+}, the colour of the orange-emitting cells immediately turned green (Figure 4.10.d). These results suggested that the probe has good cell permeability and the potential to visualize Au^{3+} levels in living cells.

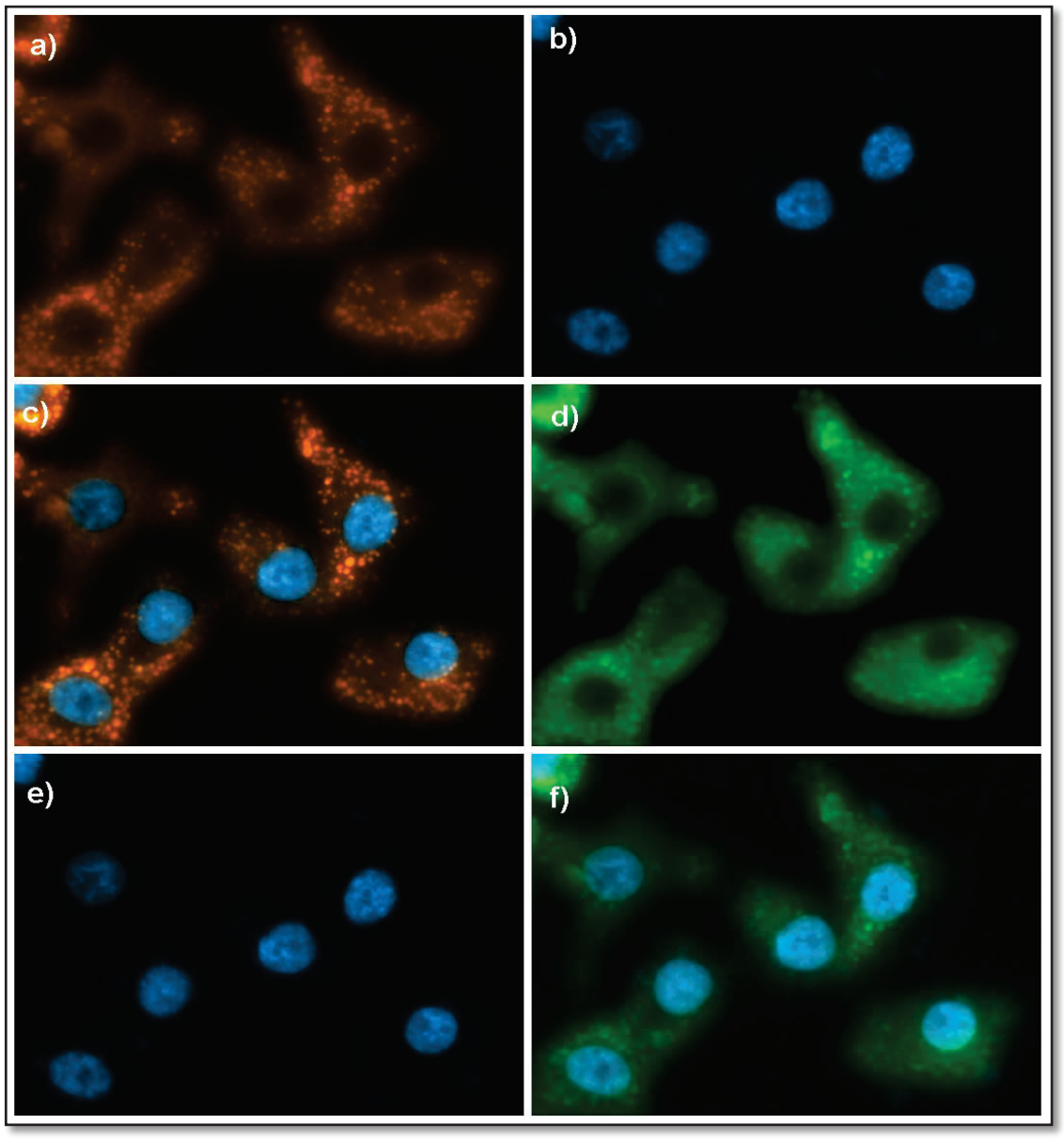

Figure 4.10. Fluorescence images of human lung adenocarcinoma cells (A549).(a) Fluorescence image of A549 cells treated with only BOD-EN (10 μM);(b and e) fluorescence image of cells treated with DAPI (control);(d) fluorescence image of cells treated with BOD-EN (10 μM) andAu^{3+}(10 μM); (c and f) merged images of frames (a and b) and (d and e).(λ_{ex}: 460 nm).

CHAPTER 5

CONCLUSION

In summary, a new fluorescent probe that shows a ratiometric fluorescence response for the detection of Au^{3+} species was developed with high sensitivity and selectivity over other metal ion species. İn this probe, BODIPY dye was used as a fluorophore and derivatized with an enynol structure, which is a reactive motif. By activating the triple bond of the gold ions, it has become selective to the gold ions as a result of non-reversible intramolecular cycling.

Thanks to the intramolecular cyclization pathway, the high wavelength probe structure is transformed into a non-conjugated BODIPY-furan structure with low wavelength. This probe showed rapid response time and high sensitivity and selectivity over other metal ion species. The probe also showed a good linear relationship between fluorescence intensity and the concentration of Au^{3+}ranging from 0 to 100μM and the detection limit was determined to be 358 nM. Fluorescence quantum yields of synthesized probe molecules were determined as $\Phi_{F(BOD\text{-}EN)= 0.148}$, $\Phi_{F(BOD\text{-}FUR)} =0.303$.

Cell-imaging applications for monitoring Au^{3+} ions in solutions and living cells were studied successfully in human lung adenocarcinoma (A549) cells. Intense fluorescence in the orange channel was observed in the cells before the addition of gold species. When the cells were incubated with Au^{+3}, the orange fluorescence intensity of the cell turned green. It was indicated that the probe is cell-permeable and can respond rapidly to Au^{3+} in living cells.

REFERENCES

Cao, X.; Lin, W.; Ding, Y. 2011. "Ratio-Au: A FRET-based fluorescent probe for ratiometric determination of gold ions and nanoparticles." *Chemistry - A European Journal*., 17(33):9066-9069.Doi: 10.1002/chem.201003586.

Choi, Ji Young; Kim, Gun-Hee; Guo, Zhiqian; Lee, Hye Yeon; Swamy, K. M. K.; Pai, Jaeyoung; Shin, Seunghoon; Shin, Injae; Yoon, Juyoung. 2013. "Highly selective ratiometric fluorescent probe for Au^{3+} and its application to bioimaging." *Bıosensors & Bıoelectronıcs;* Nov 15 2013; 49; p438-p441.Doi: 10.1016/j.bios.013.05.033.

Çetintaş, Ceyla; Karakuş, Erman; Üçüncü, Muhammed; Emrullahoğlu, Mustafa. 2016. "A fluorescein-based chemodosimeter for selective gold(III) ion monitoring in aqueous media and living systems." *Sensors & Actuators: B. Chemical*. 29 October 2016 234:109-114. DOI: 10.1016/j.snb.2016.04.158.

Das, S.; Grewal, A.S.; Banerjee, M. 2011. "A Brıef Revıew: Heavy Metal And Theır Analysis. " *International Journal of Pharmaceutical Sciences Review and Research*, 11(1):13-18.

Dong, Ming; Wang, Ya-Wen; Peng, Yu. 2010. "Highly Selective Ratiometric Fluorescent Sensing for Hg^{2+} and Au^{3+}, Respectively, in Aqueous Media." *Organıc Letters*; Nov 19 2010; 12; 22; p5310-p5313.Doi: 10.1021/ol1024585.

Emrullahoğlu, M; Üçüncü, M.; Karakuş. 2015. "A Ratiometric Fluorescent Probe for Gold and Mercury Ions." *A European Journal*, 1 September 2015, 21(38):13201-13205. Doi: 10.1002/chem.201502411.

Emrullahoğlu, M; Üçüncü, M.; Karakuş. 2015. "A BODIPY/pyridine conjugate for reversible fluorescence detection of gold(III) ions." *New Journal Of Chemıstry*; 2015; 39; 11; p8337-p8341. DOI: 10.1039/c5nj01664a.

Emrullahoğlu, M; Üçüncü, M.; Karakuş. 2016. "A BODIPY-based fluorescent probe for ratiometric detection of gold ions: Utilization of Z -enynol as the reactive unit." *Chemical Communications*, 2016, 52(53):8247-8250. DOI: 10.1039/c6cc04100k.

Kambam, S; Wang, B; Wang, F; Wang, Y; Chen, H; Chen, X; Yin, J. 2015. "A highly sensitive and selective fluorescein-based fluorescence probe for Au3+ and its application in living cell imaging." *Sensors and Actuators B Chemical* 209:1005-1010. DOI: 10.1016/j.snb.2014.12.085.

Kim, N.H.; Huh, Y.; Kim, D.; Won, M.; Kim, J.S. 2018. "A highly sensitive and fast responsive fluorescent probe for detection of Gold(III) ions based on the AIEgen disaggregation." *Dyes and Pigments*, January 2019, 160:647-653. DOI: 10.1016/j.dyepig.2018.06.036.

Liu, YH; Song, FJ; Song, ZQ; Liu, MN; Yan, B. "Gold-catalyzed cyclization of (Z)-2-en-4-yn-1-ols: Highly efficient synthesis of fully substituted dihydrofurans and furans." *Organic Letters*; Nov 24 2005; 7; 24; p5409- p5412 . DOI: 10.1021/ol052160r.

Loudet, A.; Burgess, K. 2007. "BODIPY Dyes and Their Derivatives: Syntheses and Spectroscopic Properties. " *Chem. Rev*. 2007, 107, 4891-4932. Doi: 10.1021/cr078381n.

Ozlem, S.; Akkaya, E. U. "Thinking Outside the Silicon Box: Molecular and Logic As an Additional Layer of Selectivity in Singlet Oxygen Generation for Photodynamic Therapy.". *J. Am. Chem. Soc.* 2009, 131, 48-49.

Sauer, R.; Turshatov, A.; Baluschev, S.; Landfester, K. "One-Pot Production of Fluorescent Surface-Labeled Polymeric Nanoparticles via Miniemulsion Polymerization with Bodipy Surfers." *Macromolecules* 2012, 45, 3787–3796.

Singha, S.; Kim, D.; Seo, H.; Cho, S.W.; Ahn, K.H. 2015. "Fluorescence sensing systems for gold and silver species."*Chem. Soc. Rev.***,** 2015,44, 4367. doi: 10.1039/c4cs00328d.

Srisuratsiri, Pailin; Kanjanasirirat, Phongthon; Chairongdua, Arthid; Kongsaeree, Palangpon 2017. "Reversible rhodamine-alkyne Au^{3+}-selective chemosensor and its bioimaging application." *Tetrahedron Letters*; AUG 9 2017; 58; 32; p3194-p3199. DOI: 10.1016/j.tetlet.2017.07.014.

Treibs, A.; Kreuzer, F. "Difluorboryl-Komplexe von Di- and Tripyrrylmethenen." Justus Liebigs Ann. Chem. 1968, 718, 208-223. Doi: 10.1002/jlac.19687180119.

Zhou, Wenchao; Guo, Hongyu; Lin, Jianrong; Yang, Fafu. 2018. “Multiple BODIPY derivatives with 1,3,5-triazine as core: balance between fluorescence and numbers of BODIPY units. ” *Journal Of The Iranıan Chemıcal Socıety*; 2018, 15 11, p2559-p2566, 8p.Doi: 10.1007/s13738-018-1444-6.

Wang, Enze; Pang, Lanfang; Zhou, Yanmei; Zhang, Junli; Yu, Fang; Qiao, Han; Pang, Xiaobin. 2016. “A high-performance Schiff-base fluorescent probe for monitoring Au^{3+} in zebrafish based on BODIPY.” *Biosensors and Bioelectronics*.15 March 2016 77:812-817.Doi: 10.1016/j.bios.2015.10.051

APPENDIX A

^{1}H NMR AND ^{13}C NMR SPECTRUMS OF COMPOUNDS

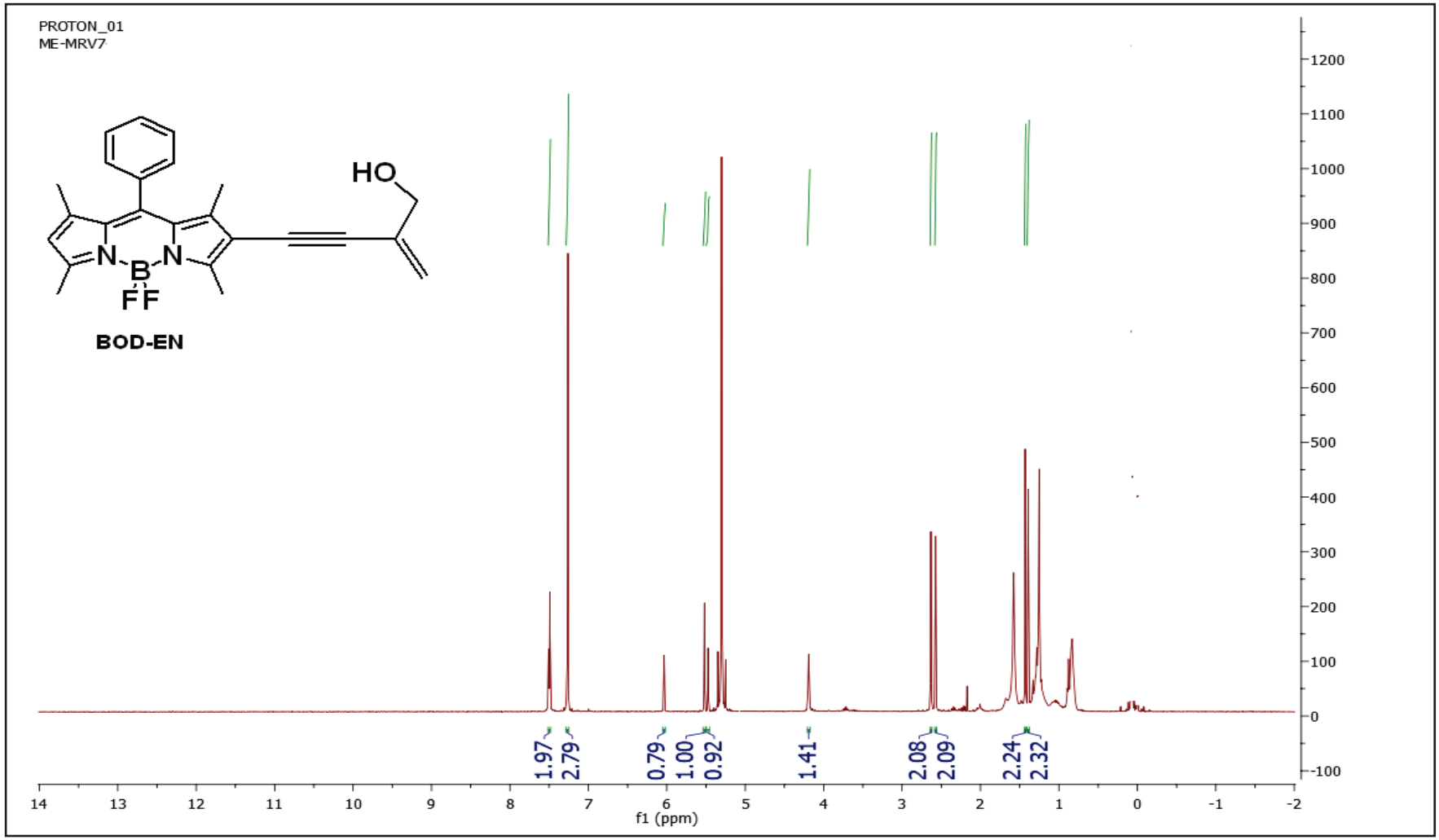

Figure A.1. ^{1}H NMR of 4-(5,5-difluoro-1,3,7,9-tetramethyl-10-phenyl-5H-5l4,6l4-dipyrrolo[1,2-c:2',1'-f][1,3,2]diazaborinin-2-yl)-2-methylenebut-3-yn-1-ol

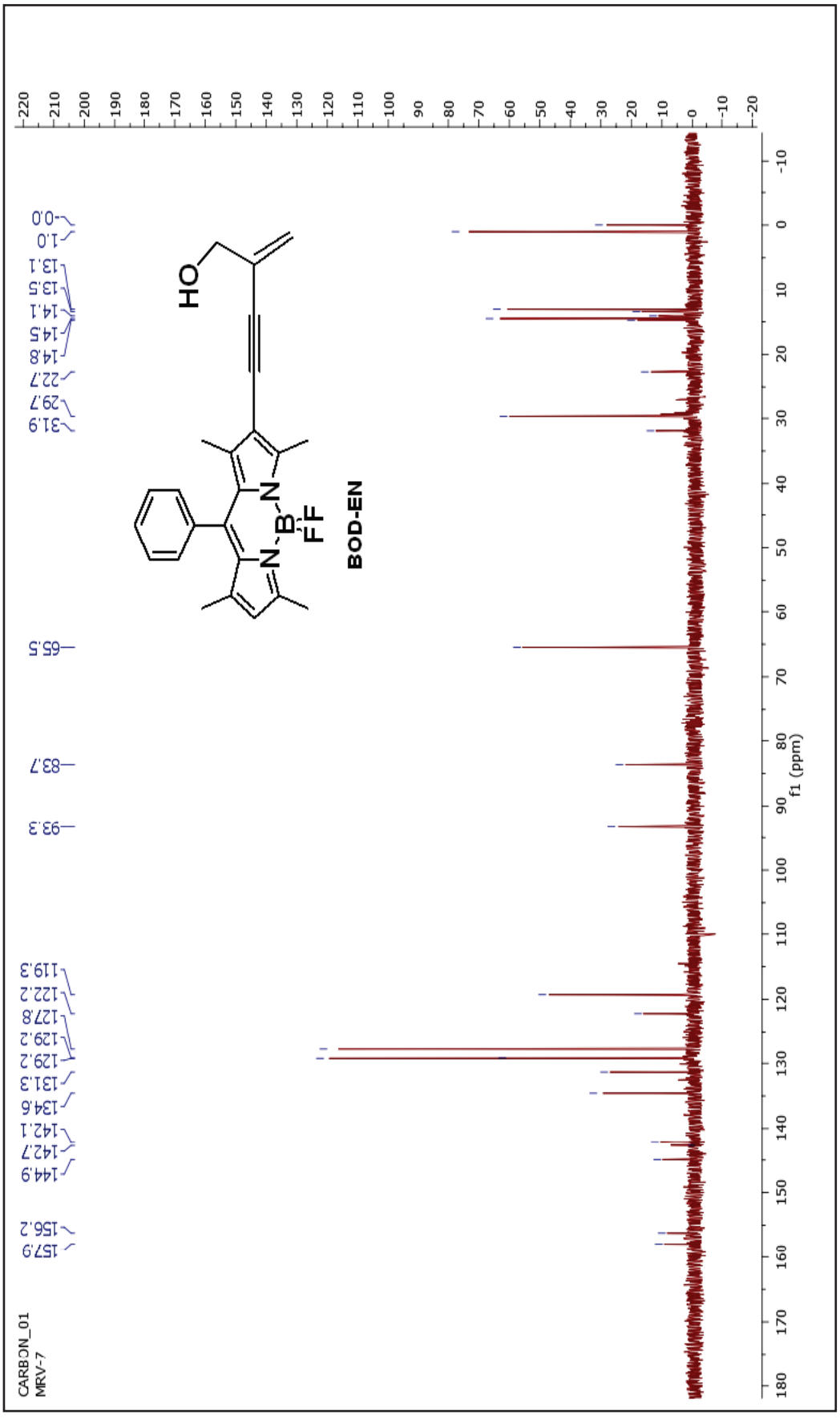

Figure A.2. ^{13}C NMR of 4-(5,5-difluoro-1,3,7,9-tetramethyl-10-phenyl-5H-5l4,6l4-dipyrrolo[1,2-c:2',1'-f][1,3,2]diazaborinin-2-yl)-2-methylenebut-3-yn-1-ol

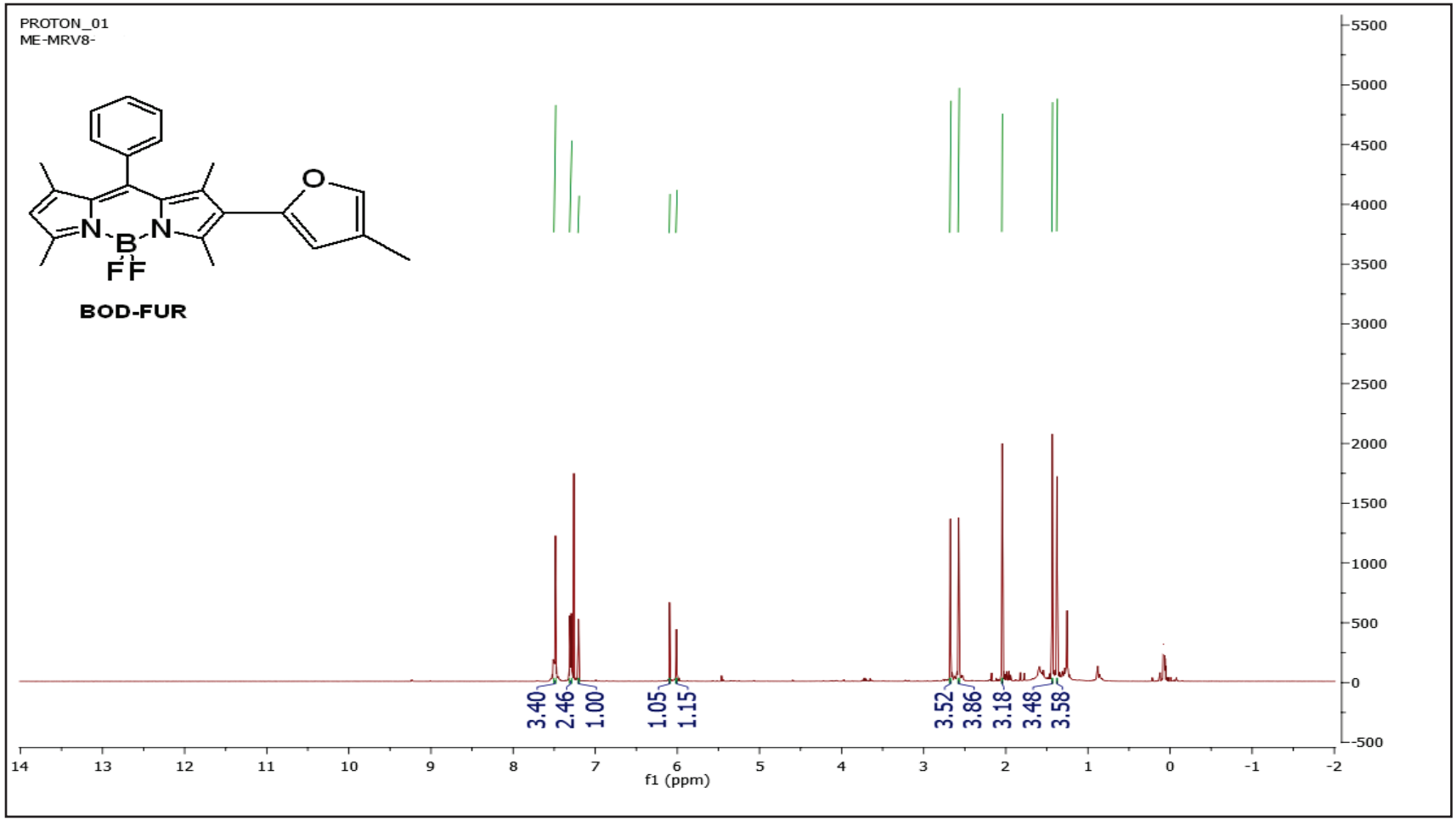

Figure A.3. ^{1}H NMR of 5,5-difluoro-1,3,7,9-tetramethyl-2-(4-methylfuran-2-yl)-10-phenyl-5H-5l4,6l4-dipyrrolo[1,2-c:2',1'-f][1,3,2]diazaborinine

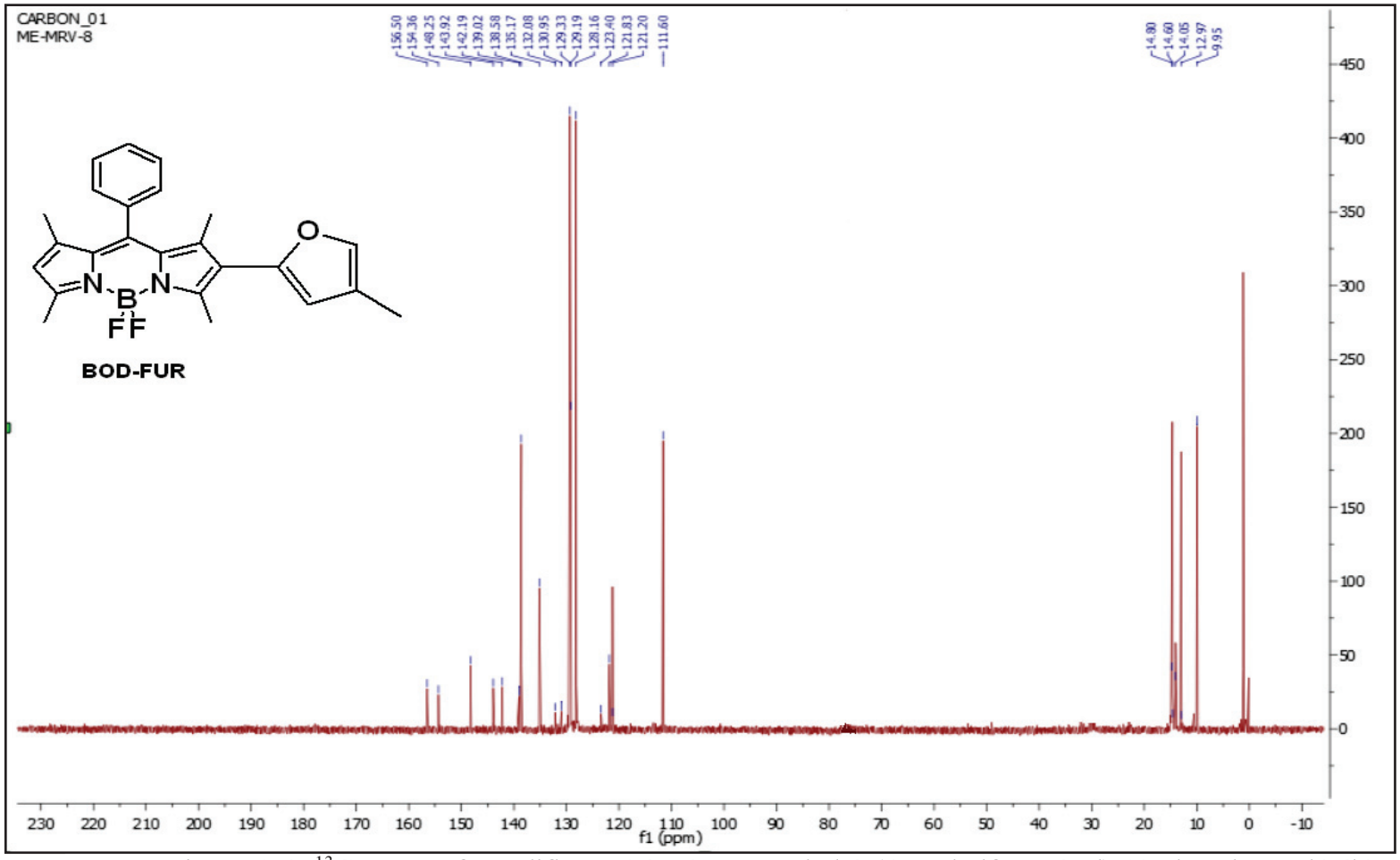

Figure A.4. ^{13}C NMR of 5,5-difluoro-1,3,7,9-tetramethyl-2-(4-methylfuran-2-yl)-10-phenyl-5H-5l4,6l4-dipyrrolo[1,2-c:2',1'-f][1,3,2]diazaborinine

APPENDIX B

MASS SPECTRUMS OF COMPOUNDS

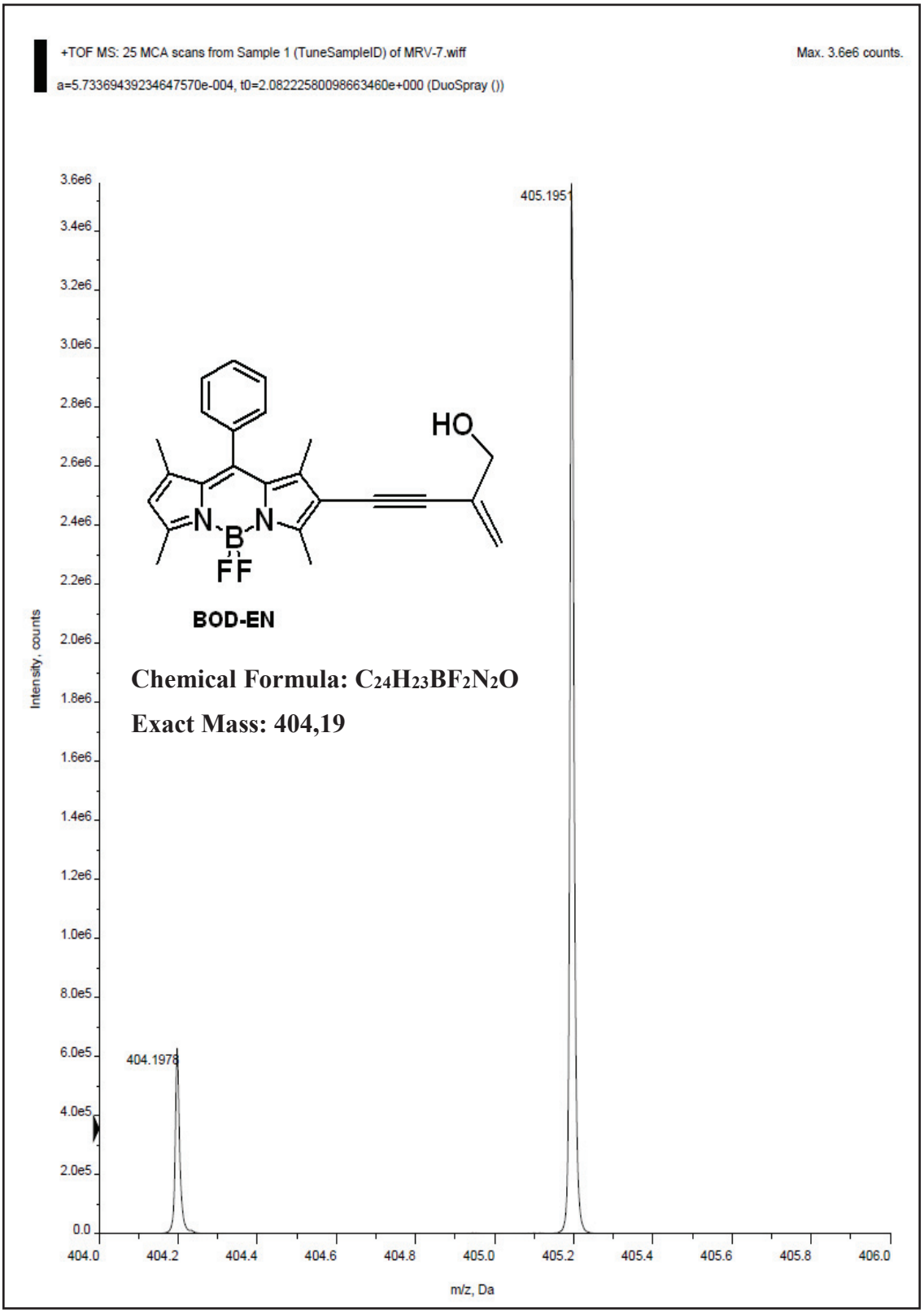

Figure B.1. Q-TOF Spectra of BOD-EN , 4-(5,5-difluoro-1,3,7,9-tetramethyl-10-phenyl-5H-5,6-dipyrrolo[1,2-c:2',1'-f][1,3,2]diazaborinin-2-yl)-2-methylenebut-3-yn-1-ol

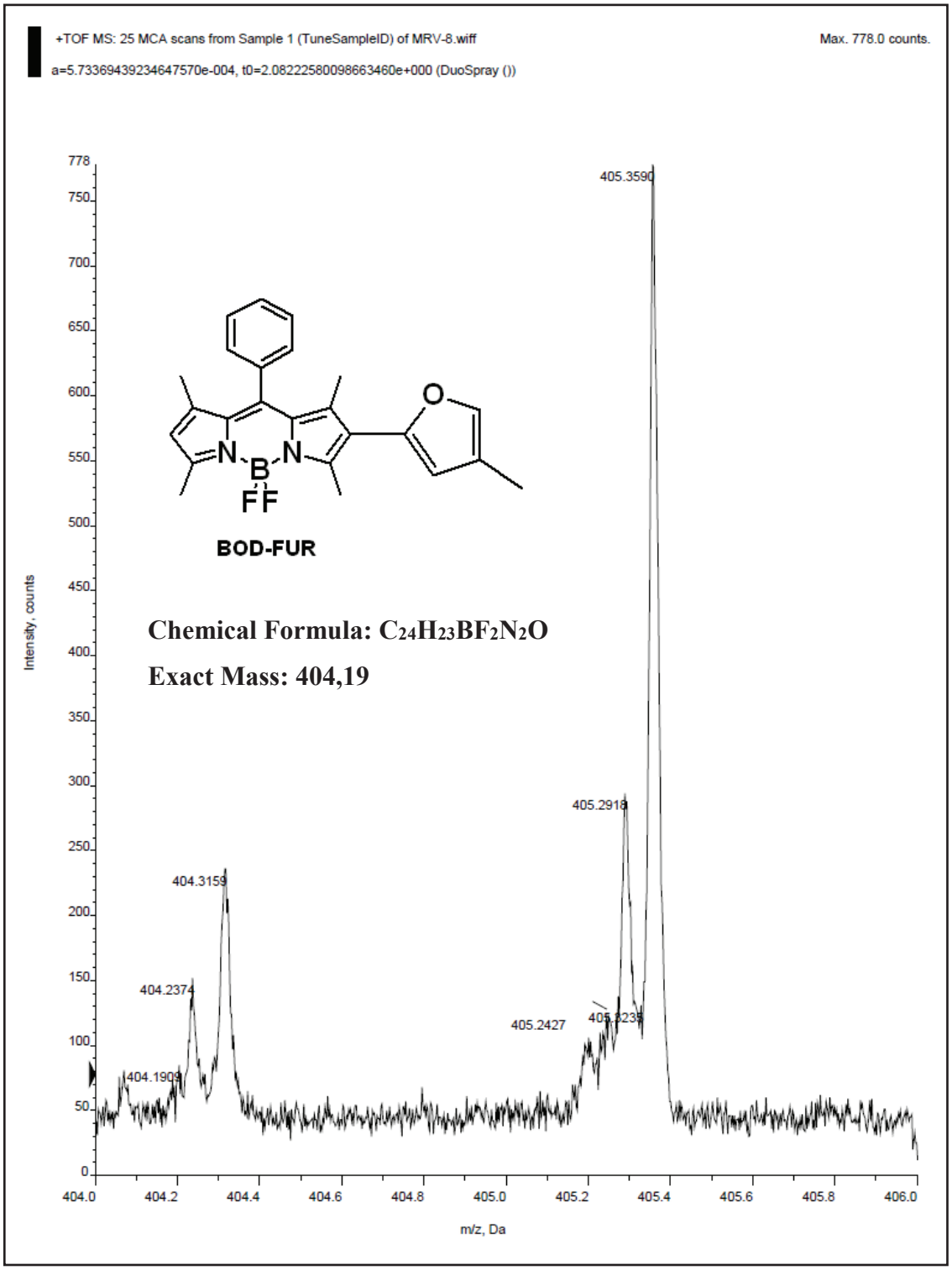

Figure B.2. Q-TOF Spectra of BOD-FUR ,5-difluoro-1,3,7,9-tetramethyl-2-(4-methylfuran-2-yl)-10-phenyl-5H-5,6-dipyrrolo[1,2-c:2',1'- f] [1,3,2] diazaborinine